FADS2 Disruption Alters Expression of Neurodevelopmental Genes in a Human iPSC-Derived Model

Callum Nicholls

Presented for the award of Master of Philosophy

Cardiff University

January 2025

Summary

Long-chain polyunsaturated fatty acids (long-chain PUFAs) are increasingly known to be important for nervous system development and function, and disruptions in the endogenous synthesis of long-chain PUFAs have been implicated as contributing to the risk of developing neuropsychiatric disorders. However, the mechanisms by which long-chain PUFA metabolism influences neurodevelopment remain poorly understood. Here, I generated mutant human induced pluripotent stem cells (iPSCs) with reduced expression of the PUFA-metabolising enzyme FADS2 and differentiated them into cortical glutamatergic neurons using dual SMAD inhibition. These mutants showed altered expression of key developmental markers, including reduced FOXG1 expression during differentiation and altered expression of MAP2 and synaptic genes at 70 days. Furthermore, I observed changes in expression of markers associated with excitatory and inhibitory activity, highlighting potential avenues for further investigation into neuronal dysfunction in this model. These findings provide potential new directions for research into the role of long-chain PUFA metabolism in neurodevelopment and offer a foundation for exploring its contribution to neuropsychiatric diseases.

Contents

Summary i

Contents ii

Acknowledgements iv

Introduction 1

FADS2 and Long-Chain PUFA Synthesis 2

Roles of Long-Chain PUFAs in the Developing and Mature Brain 4

PUFAs and the Promotion of Neurodevelopment 6

PUFAs and Cell Proliferation 8

PUFAs as Neuroprotectors 8

PUFAs and Synaptic Function 10

Long-Chain PUFA Metabolism in Neuropsychiatric Disease 11

Serum and Postmortem Tissue Samples 11

Genetic Associations 12

Utilisation of a FADS2 Mutant Stem Cell Model .....**Error! Bookmark not defined.**

Methods 14

Culture of iPSCs 14

Differentiation of iPSCs to Cortical Glutamatergic Neurons 14

Generation of Mutant iPSC Lines Via CRISPR-Cas9 16

Genotyping 17

Analysis of Gene Expression Via RT-qPCR 18

Analysis of Protein Expression by Immunoblotting 19

Data Analysis 20

Results 21

CRISPR Stem Cell Populations Exhibit FADS2 Mutation and Corresponding Reduction in Gene Expression 21

FADS2 Mutants Express Normal Levels of FADS1 But Altered Levels of COX Enzymes 24

FADS2 Mutant B Exhibits Increased NANOG Expression Compared to Control Cells 25

FADS2 Mutants Show Decreased MKI67 Expression at the Neural Progenitor Stage 27

Gene and Protein Expression of Neural Progenitor Marker Foxg1 are Decreased in FADS2 Mutants 28

FADS2 Mutant Shows a Trend Towards Decreased Generation of MAP2-Positive Cells but Increased Synaptic Marker Expression 29

Excitatory and Inhibitory Marker Expression is Altered in FADS2 Mutant Neurons at D70 32

Discussion 34

FADS2 Mutation Does Not Directly Impact Stem Cell Proliferation 34

FOXG1 Protein Levels Are Reduced in FADS2 Mutants 35

FADS2 Mutants Exhibit A Trend Towards Reduced MAP2 Expression and Upregulated Synaptic Gene Expression at D70 36

Excitatory and Inhibitory Marker Expression is Altered in FADS2 Mutant Neurons 37

Limitations of the Present Study .....**Error! Bookmark not defined.**

Conclusions 39

References 40

Supplemental 49

Acknowledgements

With thanks to my supervisor, Prof Adrian Harwood, for giving me the opportunity to work in your lab and for supporting my transition into research. Special thanks to Dr Karolina Dec for your invaluable mentorship, day-to-day support, and patience.

To my partner, Elizabeth Ferris, thank you for encouraging me to pursue research, helping me believe in myself, and providing unending support.

This work is dedicated to my grandfather, Alan Butcher, who inspired my love of science as a child and whose generous financial support made this possible.

Introduction

Dietary polyunsaturated fatty acids (PUFAs) are essential for human cellular processes and have been shown to play crucial roles in the development and function of the brain and nervous system (Bazinet and Layé, 2014). Their importance is particularly relevant to modern medicine given the increasing worldwide predominance of what is often referred to as the 'western diet', featuring PUFA compositions at odds with those consumed in our evolutionary past (Cordain et al., 2005). Furthermore, associations between altered PUFA metabolism and neuropsychiatric diseases such as bipolar disorder (Mullins et al., 2021) and schizophrenia (Yang et al., 2017) highlight the need for further research in this area, with understanding of underlying disease mechanisms in short supply.

FADS2 is a gene encoding a key enzyme involved in the metabolism of dietary PUFAs to bioactive derivatives in humans (Marquardt et al., 2000). In the present work, I aimed to study the effects of impaired PUFA metabolism on neurodevelopment *in vitro* via the generation of mutant induced pluripotent stem cells (iPSCs) lacking one copy of the FADS2 gene. Upon verifying the genotypic status of mutant cell populations, I differentiated them into cortical glutamatergic neurons via an optimised version of a standard dual SMAD inhibition protocol (Shi et al., 2012). I then performed a range of analyses of gene expression and protein levels at various key time points in the neurodevelopmental process, with a view to addressing the following questions:

1. Does a FADS2 heterozygous knockout cause corresponding changes in LC-PUFA metabolism?
2. Are there any changes in the expression of established markers of pluripotency and proliferation in FADS2 mutant stem cells?
3. Do FADS2 mutant cells exhibit detectable changes in expression of key neurodevelopmental regulators at the neural progenitor cell stage?
4. Do neuronal cell populations derived from FADS2 mutant neural progenitors exhibit changes in synaptic gene expression and alterations in excitatory/inhibitory marker expression?

FADS2 and Long-Chain PUFA Synthesis

Fatty acid desaturase 2 (FADS2) encodes the acyl-CoA 6-desaturase protein and is located on chromosome 11q12.2, alongside the related genes FADS1 and FADS3, with which it shares significant homology, including a similar exon structure (Marquardt et al., 2000). The FADS2 gene product, together with the acyl-CoA 5-desaturase encoded by FADS1, plays a pivotal role in synthesizing biologically important long-chain polyunsaturated fatty acids (PUFAs), including dihomo-γ-linolenic acid (DGLA), arachidonic acid, eicosapentaenoic acid (EPA), and docosahexaenoic acid (DHA), from shorter dietary 'precursor' PUFAs (Horrobin, 1993). These enzymes, in coordination with fatty acid elongases, sequentially elongate the shorter PUFAs and introduce additional carbon-carbon double bonds in their hydrocarbon chains. These reactions occur in the endoplasmic reticulum (Brenner, 2003). The resulting long-chain PUFAs are then incorporated into cell membranes as components of phospholipids or are metabolised into various bioactive derivatives, including eicosanoids (e.g., prostaglandins and leukotrienes), specialised pro-resolving mediators, and endocannabinoids (Bazinet and Layé, 2014). FADS1 and FADS2 are ubiquitously expressed, with the highest expression levels found in the adrenal gland as well as the brain (Uhlén et al., 2015). At the cellular level, FADS1 and FADS2 are especially highly enriched in astrocytes, but also exhibit robust expression levels in neurons and other glial cells (Siletti et al., 2023).

FADS1 and FADS2 act on two principal groups of PUFAs known as n-3 and n-6 (often also termed ω-3 and ω-6) (Calder and Grimble, 2002); this nomenclature refers to the position of the first carbon-carbon double bond from the methyl end of their hydrocarbon chains. N-3 and n-6 PUFAs are so grouped because they share similar biological properties. The n-3 α-linolenic acid and the n-6 linoleic acid are required for the synthesis of long-chain PUFAs in the FADS1 and FADS2 pathway (Wiktorowska-Owczarek et al., 2015). These PUFAs, often called essential fatty acids, cannot themselves be synthesised from monounsaturated fatty acids in mammals and must therefore be obtained through the diet (Calder, 2012). Importantly, mammals also cannot interconvert n-3 and n-6 PUFAs, and therefore the ratio of n-3 and n-6 PUFAs taken in through the diet is preserved in the body

(Lee et al., 2016). This is key when considering the impacts of modern diets on health; excess n-6 PUFAs, as are commonly seen in the modern western diet, have been repeatedly associated with negative health outcomes, while n-3 PUFAs are generally seen as protective (Schmitz and Ecker, 2008).

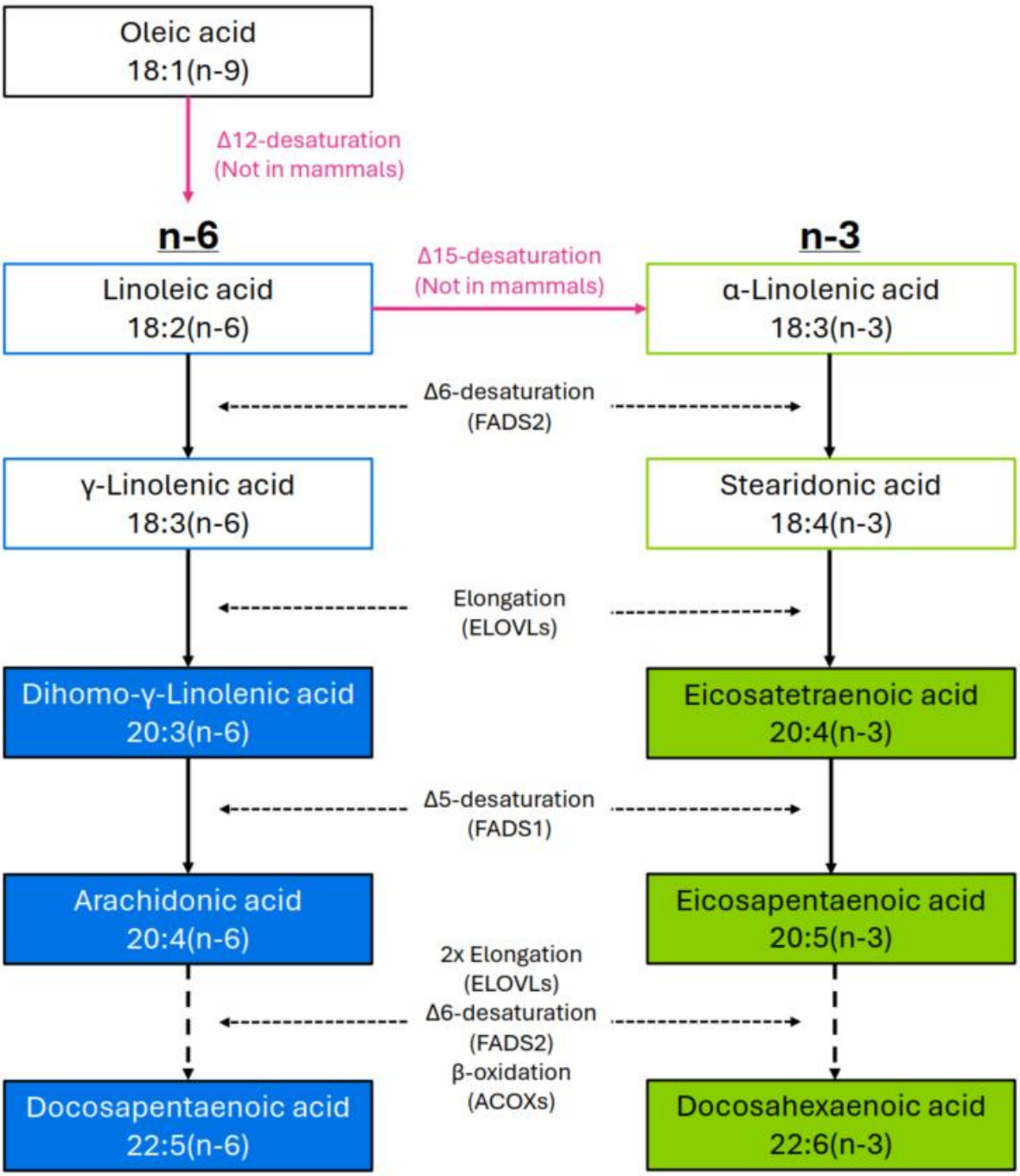

Fig 1: Long-Chain PUFA Synthesis. Biologically important long-chain PUFAs (filled boxes) including arachidonic acid, EPA, and DHA are synthesised from shorter dietary precursor PUFAs by a suite of enzymes including FADS1, FADS2, elongases, and acyl-CoA oxidases. These fatty acids are then incorporated into phospholipid bilayers or metabolised into

bioactive derivatives including eicosanoids, endocannabinoids, and SPMs. Importantly, mammals cannot synthesise PUFAs from saturated or monounsaturated fatty acids and cannot interconvert n-6 and n-3 PUFAs.

Roles of Long-Chain PUFAs in the Developing and Mature Brain

The functions of long-chain PUFAs, particularly arachidonic acid and DHA, in the brain are numerous. They are ubiquitous organism wide as constituents of plasma membrane phospholipids and are especially prevalent in this fashion in the brain (Bazinet and Layé, 2014). In this role, PUFAs confer specific biophysical properties on both cell and nuclear membranes that support their proper functions, regulating their fluidity, elasticity, and thickness (Baccouch et al., 2023; Jacobs et al., 2021; Romanauska and Köhler, 2023). Furthermore, when required, long-chain PUFAs can be liberated from membrane phospholipids through the actions of phospholipases A1 and A2 and utilised for the synthesis of bioactive oxylipins and endocannabinoids (Bazinet and Layé, 2014). Oxylipins, including the eicosanoids, exert systemic hormone-like effects such as regulating inflammation and serve multiple functions in the brain (Calder, 2020), while the endocannabinoids serve as a class of neurotransmitters activating specific G-protein coupled receptors (GPCRs) known as cannabinoid receptors at synapses (Wilson and Nicoll, 2002). In general, both n-3 and n-6 PUFAs are essential for proper brain function, although most research focusses on the beneficial effects of n-3 PUFAs (Calder, 2012); what is apparent is that in many cases the ratio of n-6:n-3 PUFAs must be finely regulated, with imbalanced ratios leading to negative health outcomes (Simopoulos, 2002).

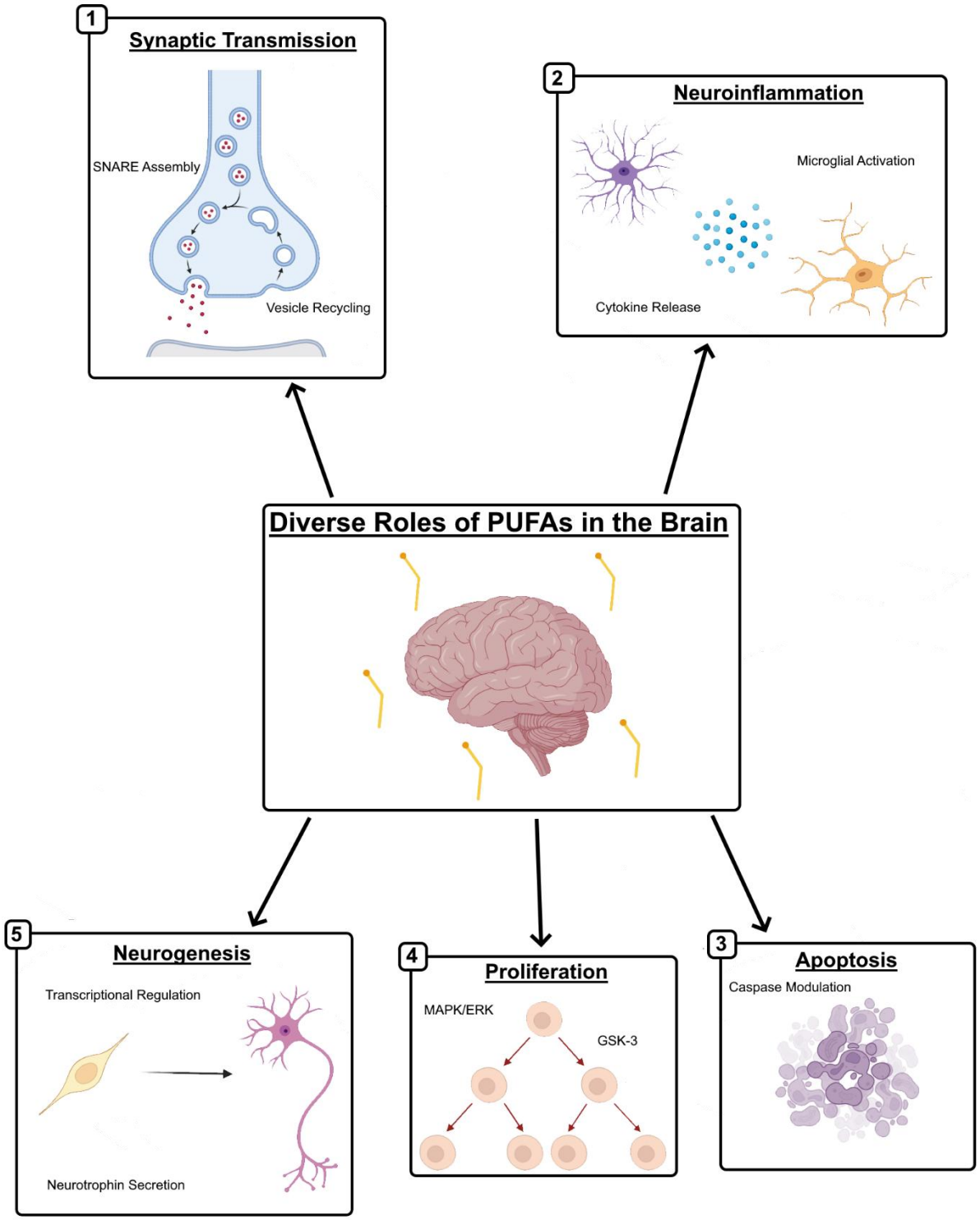

Fig 2: Diverse Regulatory Roles of PUFAs in the Brain. Long-chain PUFAs have been reported to influence a multitude of processes within the brain, including synaptic transmission, neuroinflammation, neurodevelopment, cell proliferation, and apoptosis. Their effects are mediated by a wide range of signals and interactions.

PUFAs and the Promotion of Neurodevelopment

Long-chain PUFAs are highly important for neurodevelopment and the formation of functioning neuronal networks, with the beneficial effects of n-3 PUFAs being particularly significant (Bazinet and Layé, 2014). Culturing primary rat cortical neurons in medium containing 25μM DHA increases the average neurite length and branch number of the cell populations (Cao et al., 2005). This effect is notably lost at both lower and higher concentrations, with high concentrations of DHA producing detrimental effects. Work in numerous model systems describes n-3 long-chain PUFAs as promoting neuronal differentiation. Culture of 15-day old primary rat neural stem cells in the presence of DHA significantly increases the number of Tuj-1-positive neurons generated after 7 days, and *in vivo* dietary supplementation in rats also increases creation of newborn NeuN-positive cells (Kawakita et al., 2006). Tuj-1 (tubulin beta 3, TUBB3), a neuron-specific cytoskeletal protein, and NeuN (RBFOX3), an mRNA splicing regulator, are well established markers of early and late neurons (Menezes and Luskin, 1994; Duan et al., 2016). This result was also replicated in adult lobsters, where supplementing the n-3 PUFA precursor α-linolenic acid to increase the dietary ratio of n-3 to n-6 PUFAs increased the proliferation of neural stem cells *in vivo* (Beltz et al., 2007). Another elegant study made use of transgenic mice expressing the *Caenorhabditis* fat-1 gene, which enables conversion of n-6 PUFAs to n-3 PUFAs (Kang et al., 2004). These mice exhibit increased hippocampal neurogenesis, dendritic spine density, and neurite outgrowth compared to wildtype mice, and perform better on a standard test of spatial learning (He et al., 2009). Furthermore, mice embryonic stem cells proliferate more readily in the presence of DHA and show enhanced neurite growth when differentiated to neurons (He et al., 2009). DHA also ameliorates the differentiation of mouse induced pluripotent stem cells (iPSCs) to dopaminergic neurons *in vitro* (Chang et al., 2012).

Studies of the effects of n-6 PUFAs are less numerous and in some cases find contrasting results. One study reported that arachidonic acid increases neural cell proliferation in wildtype rats and partially rescues neurogenesis in Pax6 heterozygous mutant rats (a model of impaired neurogenesis), with these improvements translating to rescue of startle behaviour in a standard test (Maekawa et al., 2009). Both arachidonic acid and DHA have been reported to enhance the

maintenance of rat primary neural progenitor cells cultured *in vitro*, and interestingly, arachidonic acid was reported to preferentially promote astrocyte differentiation in contrast to the neuron-promoting DHA (Sakayori et al., 2011). However, in a recent study, human iPSCs were differentiated to neurons in the presence of varying ratios of n-6:n-3 precursor PUFAs. In this model, high ratios of n-6:n-3 PUFAs in the culture medium were found to decrease the expression of key neural progenitor cell markers Foxg1 and Pax6 in a dose-dependent manner (Dec et al., 2023).

Different mechanisms underpinning the effects of long-chain PUFAs on differentiation have been proposed. DHA-mediated increases in neuronal differentiation of rat neural stem cells have been associated with decreased expression of Hes1 and increased expression of NeuroD (Katakura et al., 2009); Hes1 and NeuroD are bHLH transcription factors that respectively inhibit and enhance the transcription of neuronal microtubule-associated MAP2 (Bhat, 2006). EPA has also been reported to upregulate Hes6, which inhibits the activity of Hes1 (Bae et al., 2000), and NeuroD, while arachidonic acid downregulates Hes1 (Katakura et al., 2013). In mouse iPSCs and derived dopaminergic neurons, DHA was found to upregulate Nurr1, a key regulator of dopaminergic neurogenesis (Chang et al., 2012; Decressac et al., 2013). Furthermore, DHA increased the expression of brain- and glial cell line-derived neurotrophic factors (BDNF and GDNF) in this model. Neurotrophins including BDNF and GDNF are crucial regulators of neurogenesis and synaptogenesis (Park and Poo, 2013). DHA and EPA have also both been described as increasing expression of BDNF and GDNF in human SH-SY5Y neuroblastoma cells via decreased methylation and increased hydroxymethylation in promoter regions (Zhang et al., 2018; Kou et al., 2008; Ceccarini et al., 2022). PUFAs are known to activate peroxisome proliferator-activated receptors (PPARs), particularly PPARɣ, with n-3 PUFAs demonstrating the greatest affinity (Echeverría et al., 2016). PPARs are a family of nuclear receptors that bind DNA to regulate transcription (Tyagi et al., 2011), and the role of PPARɣ in osteogenesis of mesenchymal stem cells is well established (Li et al., 2018). N-3 PUFAs have been demonstrated to promote osteogenesis via increased Akt phosphorylation at the membrane (Levental et al., 2017); PI3K/Akt activation inhibits TGF-β signalling (Remy et al., 2004), which is also well known for its importance in

generation of neural progenitor cells (Watabe and Miyazono, 2009). This therefore presents another putative mechanism by which PUFAs influence neurodevelopment.

PUFAs and Cell Proliferation

PUFAs and their metabolites are known to be important for the normal growth of cells, with most of the existing literature focussing on cancer models. Multiple studies report n-6-derived prostaglandins as inducing phosphorylation of extracellular signal-regulated kinases (MAPK/ERKs) in cancer and epithelial cells (e.g. Krysan et al., 2005). ERK phosphorylation leads to its translocation to the nucleus, where it activates multiple transcription factors that promote cell cycle progression (Sun et al., 2015). In an alternative mechanism, prostaglandin E2 (PGE2) has also been described as inducing phosphorylation of glycogen synthase kinase-3 (GSK-3), an effect mediated by protein kinase A (PKA) and phosphatidylinositol 3-kinase (PI3K) (Fujino et al., 2002). GSK-3 exerts pleiotropic effects in cells, among which is the regulation of cell proliferation (Shin et al., 2011). In human induced pluripotent stem cells, high ratios of n-6 PUFAs to n-3 PUFAs in the cell culture medium results in increased population doubling time at the stem cell stage, but decreased expression of key proliferation marker MCM2 at the neural progenitor stage (Dec et al., 2023).

PUFAs as Neuroprotectors

In mature neurons, PUFAs can also regulate apoptosis, though their effects appear to be contrasting depending on the cell type investigated. In neural cells, DHA has been described as anti-apoptotic. In mouse neuroblastoma cells, DHA supplementation leads to its accumulation in membrane phosphatidylserine and resulting Raf-1 translocation and downregulation of caspase-3 (Kim et al., 2003; Kim et al., 2010). Raf-1 promotes cell survival by inhibiting apoptosis signal-regulating kinase 1 (ASK1) (Chen et al., 2001). Comparable findings have been observed for both DHA and EPA, as demonstrated in human neuroblastoma cells (Zhang et al., 2018) and an *in vivo* rat model of traumatic brain injury. In the latter, the effect was attributed to enhanced neuronal autophagy driven by SIRT1-mediated deacetylation of Beclin-1, which reduces its nuclear export (Chen et al., 2018); Beclin-1 inhibits the maturation of functional autophagosomes (Kang et al., 2011). The n-3 docosapentaenoic acid (DPA) has also been reported to reduce microglial activation in a rat model of aging (Kelly et al., 2011).

Research also highlights the role of n-3 PUFAs in protection against oxidative stress. EPA and DHA increase mouse neural progenitor cell viability when incubated in hydrogen peroxide, and transgenic mouse neural progenitor cells expressing *Caenorhabditis* fat-1 also exhibit increased resilience to oxidative stress (Liu et al., 2014). These effects were accompanied by increased expression of nuclear factor erythroid 2–related factor 2 (Nrf2), a transcription factor that regulates the expression of multiple antioxidant genes (Ma, 2013).

N-3 long-chain PUFAs, particularly DHA, give rise to a class of derivative molecules known as specialised pro-resolving mediators (SPMs) that are key in the resolution o inflammation (Basil and Levy, 2016). One such SPM, neuroprotectin D1 (NPD1), is well established as preventing neuronal death, for example in the face of amyloid beta 42 (Aβ42) insult (Stark and Bazan, 2011). NPD1 also protects against oxidative stress in retinal pigment epithelial (Mukherjee et al., 2004) and human neural cells (Lukiw et al., 2005) via upregulation of the antiapoptotic Bcl-2 and Bcl-xl and inhibition of caspase-3. NPD1 appears to inhibit pathological cleavage of amyloid precursor protein by β-secretase 1, an effect that is PPARγ-dependent (Zhao et al., 2011).

Multiple studies associate n-3 PUFA consumption with decreased levels of pro-inflammatory cytokines in the brain. In rats, supplementation with EPA attenuates IL-1β-induced upregulation of microglial marker CD11b and astrocyte marker GFAP and downregulates proinflammatory cytokine TNF-α (Dong et al., 2018). Furthermore, EPA upregulated expression of BDNF and its receptor tropomyosin receptor kinase B (TrkB), but reduced expression of p75 neurotrophin receptor (p75NTR), reversing the effects of Il-1β challenge. In fat-1 transgenic mice, immune challenge by lipopolysaccharide (LPS) results in attenuated increases in gene expression of multiple inflammatory markers including IL-6, CCL3, CCL2 and TNF-α, as well as microglial markers Iba1, CD11b and CD45 (Orr et al., 2013). Feeding wildtype mice a diet rich in n-3 PUFAs was sufficient to bring wildtype inflammation in line with the fat-1 condition. N-3 PUFA effects on microglial activation have also been attributed to increased activity of SIRT1 (Inoue et al., 2017).

PUFAs and Synaptic Function

Long-chain PUFAs including arachidonic acid and DHA also play important roles in neuronal function, particularly at synapses. Arachidonic acid is the principal precursor of the endocannabinoids, a key group of retrograde synaptic messengers including N-arachidonoylethanolamine (AEA, anandamide) and 2-arachidonoylglycerol (2-AG), so named because their receptors are also the target of tetrahydrocannabinol, the principal psychoactive component of cannabis (Wilson and Nicoll, 2002). Endocannabinoids have been implicated in multiple forms of synaptic plasticity, including short-term depolarisation-induced depression of inhibition (DSI) and excitation (DSE), and long-term depression (LTD), via the action of the CB1 and CB2 receptors (Castillo et al., 2012). 2-AG is synthesised by diacylglycerol lipase α (DGLα), which acts on diacylglycerol liberated from plasma membranes by calcium-dependent activation of phospholipase Cβ (PLCβ), and travels backwards across the synaptic cleft to activate presynaptic CB receptors (Castillo et al., 2012). AEA synthesis is less well understood but involves N-acyl-phosphatidylethanolamine-hydrolysing phospholipase-D (NAPE-PLD) (Castillo et al., 2012). As well as being directly synthesised from the n-6 arachidonic acid, endocannabinoid levels are directly modulated by dietary PUFA content, including n-3 PUFAs. In one study, mouse deficient in brain DHA were found to have impaired endocannabinoid signalling resulting in anxiety-related behaviours (Larrieu et al., 2012). Other authors reported that n-3 PUFA-deficient mice did not have altered endocannabinoid levels, but that endocannabinoid-mediated synaptic plasticity was completely ablated due to decoupling of CB1 from its effector $G_{i/o}$ proteins; this was accompanied by altered emotional behaviour (Lafourcade et al., 2011).

PUFAs also play key roles in synaptic vesicle dynamics, which are essential for neurotransmission at synapses. During neurotransmission, neurotransmitters contained in synaptic vesicles are exocytosed from the presynaptic neuron, after which vesicle components are endocytosed from the membrane via the clathrin-mediated pathway and recycled to avoid *de novo* synthesis and sustain high levels of release. Phosphoinositides, phosphorylated phosphatidylinositols ordinarily containing long-chain PUFAs, are key regulators of both exocytosis and endocytosis, as well as ER-Golgi trafficking of COP-coated vesicles (Posor et al., 2022). These

lipids serve to spatiotemporally coordinate and direct the complex protein machineries involved in these essential cellular processes (Posor et al., 2022). Accordingly, alterations in n-6 and n-3 PUFA levels appear to affect these processes. PUFAs with a greater carbon chain length and higher degree of unsaturation appear to enhance synaptic vesicle endocytosis (Pinot et al., 2014). Levels of arachidonic acid also appear to modulate formation of the soluble NSF-attachment protein receptor (SNARE) complex fundamental to exocytosis in a dose-dependent manner in chromaffin cells (Latham et al., 2007); arachidonic acid also appears to interact with Munc18 in SNARE complex formation. PUFAs of a greater carbon chain length and unsaturation are more potent inducers of endocytosis than shorter and more saturated fatty acids in both mouse neuroblastoma cell lines and primary mouse neurons; PUFAs appear to cooperate with α-synuclein in inducing endocytosis (Ben Gedalya et al., 2009).

Long-Chain PUFA Metabolism in Neuropsychiatric Disease

The importance of studying long-chain PUFA metabolism and its functions is underpinned by associations between PUFA levels and neuropsychiatric disease, in particular bipolar disorder and schizophrenia.

Serum and Postmortem Tissue Samples

A multitude of studies over several decades have drawn an association between physiological levels of long-chain PUFAs and bipolar disorder. An early clinical study finding that oral treatment with n-3 PUFAs yielded greatly improved outcomes compared to placebo in bipolar patients generated significant subsequent interest (Stoll et al., 1999). An initial study found that bipolar patients have significantly reduced DHA and arachidonic acid in their erythrocyte plasma membranes (Chiu et al., 2003), however, a subsequent meta-analysis of six studies found that only DHA was robustly and significantly reduced (McNamara and Welge, 2016). A more recent study has also reported reduced arachidonic acid in circulating bipolar patient blood plasma (Ashizawa et al., 2024). Studies also report altered PUFA levels in postmortem brain tissue samples; for example, DHA and arachidonic acid deficits were reported in postmortem orbitofrontal cortex (McNamara et al., 2008). However, these results have not always been corroborated in subsequent research (Igarashi et al., 2010).

Similar results regarding altered PUFA levels have been reported in schizophrenia patients. A meta-analysis of serum studies found that DPA, DHA and arachidonic acid are all robustly decreased in schizophrenia, although as with bipolar disorder, the authors noted that results vary substantially (Hoen et al., 2013). One study highlighted specific increases in levels of n-6 PUFAs in schizophrenia patients compared with controls (Yang et al., 2017). A meta-analysis of the effects of PUFA supplementation in schizophrenia found that that there was insufficient evidence to conclude any therapeutic effects, and that more research was needed (Irving et al., 2006). A recent two-sample Mendelian randomisation study found specific risk-reducing effects of long-chain PUFA levels in schizophrenia, with no effect for precursor PUFAs (Jones et al., 2021).

Genetic Associations

Recent genome-wide association studies (GWAS) have also identified single nucleotide polymorphisms (SNPs) in the FADS2 gene as potential contributors to bipolar disorder risk. An initial study identified rs28456 in a Japanese population (Ikeda et al., 2018); these were later followed up in large European cohorts by rs12226877 (Stahl et al., 2019) and rs174592 (Mullins et al., 2021). These SNPs lie in intron regions of the FADS2 gene, suggesting that they may exert their effects through dysregulation of gene expression rather than disruption of a functional protein product. Another SNP in the FADS1/2 locus previously identified as modifying PUFA metabolism, rs174550, was found in a follow-up study to be associated with significantly reduced arachidonic acid blood plasma levels when covarying with bipolar disorder diagnosis (Ashizawa et al., 2024). Another study investigated this and two other SNPs (rs174546, rs174547), again finding significantly reduced serum arachidonic acid, but no reduction in n-3 PUFAs or oxylipin levels (Rabehl et al., 2024). However, other investigators looking into SNPs rs28456, rs174576, and rs174547 found significantly decreased EPA and DHA but significantly increased arachidonic acid and DGLA (Koga et al., 2019). These levels were also correlated with plasma IL-6 and TNF-α, suggesting a link to systemic inflammation (Koga et al., 2019). These differing results suggest heterogeneous effects of individual FADS2 SNPs on n-3 and n-6 PUFA metabolism, including the possibility of loss of function or gain of function. To model the systemic effects of

FADS2 loss of function, researchers generated heterozygous mutant mice lacking one copy of both FADS2 and FADS1 via CRISPR-Cas9 (Yamamoto et al., 2023). These heterozygous knockout mice were found to represent a robust model of bipolar disorder according to several well-established behavioural measures, with phenotypes rescuable by either long-term DHA supplementation or administration of lithium. The authors also created a conditional heterozygous deletion of FADS1 and FADS2 specific to neural lineage cells via utilisation of the Cre-Lox system under the control of a nestin driver (Yamamoto et al., 2023). In this case, it was found that behavioural phenotypes were normal, which is perhaps unsurprising when considering that brain lipid homeostasis is regulated by external supply from the blood plasma (Bazinet and Layé, 2014).

Research Aims and Objectives

Building on prior research showing that altered PUFA ratios disrupt the development of human iPSC-derived neural progenitor cells, I aimed to further explore the role of long-chain PUFA synthesis in neurodevelopment by focusing on the FADS2 gene. Specifically, I examined the differentiation of mutant iPSCs carrying a heterozygous frameshift mutation in the FADS2 gene, rendering them incapable of producing normal levels of functional FADS2 protein. The aims of this preliminary study were as follows:

1. Demonstrate the utility of a FADS2 heterozygous knockout stem cell model in studying the impairment of long-chain PUFA metabolism by examining gene expression changes in enzymes of this pathway
2. Considering previous literature linking cell proliferation and apoptosis with long-chain PUFAs, assess the expression of established transcriptomic markers of cell proliferation and pluripotency in these mutant stem cells compared to wildtype cells.
3. Differentiate these iPSCs into cortical glutamatergic neurons via an optimised version of a standard dual SMAD inhibition protocol (Shi et al., 2012) and assess the expression of key developmental marker FOXG1 and marker of proliferation MKI67 at the neural progenitor stage.
4. Finally, examine the expression of genes encoding synaptic proteins in mature neuronal cell populations derived from FADS2 mutant neural

progenitor cells, and characterise any changes in the expression of excitatory and inhibitory markers in these cells.

Methods

Culture of iPSCs

Induced pluripotent stem cells (iPSCs) were maintained in E8 (Essential 8 Medium, Gibco, A1517001) with the occasional use of E8 Flex (Gibco, A2858501). E8 is formulated on a base of DMEM/F-12 and contains negligible levels of precursor PUFAs. iPSCs were maintained on 6-well plates coated with Cultrex basement membrane (R&D Systems, 3434-005-02) in DMEM/F-12 (Gibco, 21331020) at 1% v/v. iPSCs were passaged regularly to prevent cell stress, generally falling every 2-3 days. Cells were dissociated with a variety of reagents including Versene solution (Gibco, 15040066), Gentle Cell (Stem Cell Technologies, 100-0485), or TrypLE (Gibco, 12604021) when requiring a single-cell suspension.

Differentiation of iPSCs to Cortical Glutamatergic Neurons

iPSCs were directed towards a neuronal fate utilising a modified version of a standard dual SMAD inhibition protocol (Shi et al., 2012). Cells were seeded onto a 12-well plate coated with Cultrex and maintained in E8. Once cells had reached approximately 90% confluency (around 2-3 days later), termed D0 (Day 0), the medium was switched from E8 to SBLDN medium for neural induction. SBLDN medium was prepared with 2:1 DMEM/F-12:neurobasal medium (Gibco, 21103049) supplemented with 1% B-27 without retinyl acetate (Gibco, 12587010), 1% N-2 (Gibco, 17502048), 0.15% SB-431542 (SB, APExBIO, A8249), 0.015% LDN-193189 (LDN, APExBIO, A8324), 1.5% Penicillin-Streptomycin-Glutamine (PSG, Gibco, 10378016), and 0.15% 2-mercaptoethanol (Sigma-Aldrich, M3148). B-27 contains precursor lipids but not long-chain PUFAs. SB and LDN respectively inhibit TGF-β signalling (Inman et al., 2002) and bone morphogenetic protein (BMP) signalling (Boergermann et al., 2010), specifying a neuroectodermal fate. The medium was changed regularly to prevent cell stress and maintain neural induction.

At eight days from neural induction (D8) and upon the formation of a uniform sheet of neuroepithelial cells, the cells were passaged in the ratio 2:3 onto fresh 12-well plates coated with human fibronectin (Sigma-Aldrich, FC010) in DPBS at 1.5% v/v. Cells were incubated in 0.2% Y-27632 (Y27, Biotechne, 1254) for at least one hour prior to passaging; Y27 inhibits rho-associated protein kinases (ROCKs) and reduces cell apoptosis following passaging (Ishizaki et al., 2000). Cells were dissociated with Versene and care was taken not to overly disrupt cell aggregates. Cells were given Y27 overnight after passaging, and the following day (D9), the medium was changed to N2B27 medium, prepared as with SBLDN medium without SB and LDN, to allow formation of neural progenitor cells.

Medium changes continued every other day. Rosettes, the classical morphology of neural progenitor cells, begin to become obvious at around 15 days post induction (Shi et al., 2012). At D18, cells were passaged in the ratio 1:3 onto plates coated with 10% poly-D-lysine (PDL, Gibco, A3890401) in DPBS and 1.5% mouse laminin I (Biotechne, 3401-010-02) in DPBS. Cells were again treated with Y27 for at least one hour prior to passaging and were dissociated with Versene. In this case, cell aggregates were disrupted as much as possible before plating.

At D26, the medium was changed to RA medium prepared as with N2B27 medium but with B-27 plus retinyl acetate (Gibco, 17504044) rather than B-27 without retinyl acetate. Retinyl acetate, a form of vitamin A, helps promote efficient neurogenesis (Shi et al., 2012). At D28, if judged to be overly confluent, cells were passaged a third and final time, again onto PDL and laminin substrate in ratio 1:3. This third passage was performed with accutase (Sigma-Aldrich, A6964-500ML) to create a single-cell suspension. Cells were centrifuged at 200rcf for 5mins to pellet, the supernatant was aspirated, and the cells were resuspended in medium and triturated to ensure sufficiently disrupt aggregates before plating. From this point, neurons were maintained in RA medium.

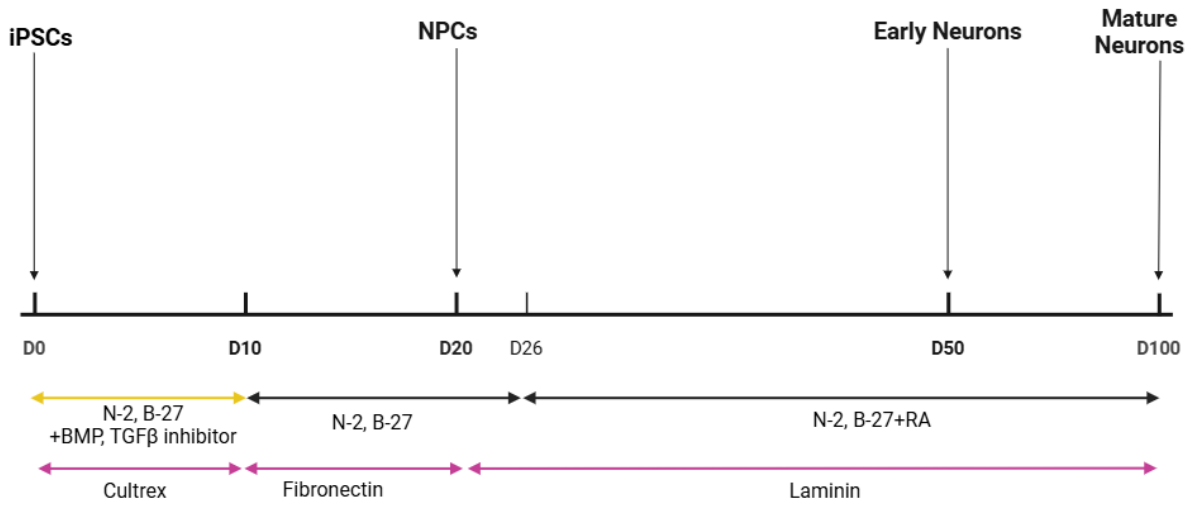

Fig 3: Dual SMAD Inhibition. To induced neuronal differentiation, iPSCs are cultured in BMP and TGB-β inhibitors until D10, when a uniform neuroepithelial sheet has formed. At D26, retinyl acetate (vitamin A) is added to the culture medium to promote efficient conversion of neural progenitor cells to neurons. By around D35, neurons are the majority cells in culture, but full mature networks do not form until D70-D100.

Generation of Mutant iPSC Lines Via CRISPR-Cas9

FADS2 mutant iPSC lines were generated using CRISPR-Cas9, performed by Dr B Kenny. Briefly, control IBJ4 stem cells were selected for Cas9 with doxycycline and transfected with crRNA and tracrRNA via lipofection. Doxycycline selection was again performed. Two pairs of guide RNA (gRNA) were used for CRISPR: TCAACAGTCAAAGATCACTGAGG and GAACCATGCAATGCTCTCCAGGG, and TCGCCCTGGAGAGCATTGCATGG and GGTGTCACGCCTCACCTGAGAGG. Both sets of guides targeted Exon 3 of all three FADS2 transcript variants. After CRISPR had been performed, wells were screened for a successful deletion using Oxford Nanopore Sequencing. Wells showing a deletion in a high number of reads were subcloned once using DNA gel electrophoresis selection, and resulting clones were assigned a name based on their position on the CRISPR plate and position on the subcloning plate e.g. (B2F4). Subcloned cells were then genotyped to verify a mutation prior to experiments.

Genotyping

Subcloned cell lines were screened for successful mutations via DNA gel electrophoresis. Cells were pelleted and genomic DNA was purified using the PureLink Genomic DNA Mini Kit (Invitrogen, K182002) or the ISOLATE II Genomic DNA Kit (Meridian Bioscience, BIO-52067). Both kits follow a similar method; in short, cell samples and nuclei were lysed by incubating in a lysis buffer containing a chaotropic agent on a thermal plate at 55C for 10mins in the presence of proteinase K and RNase A. DNA was precipitated with >95% ethanol, bound to a silica spin column membrane, washed and eluted into nuclease-free water. DNA concentration was measured by spectrophotometry (NanoDrop 8000 Spectrophotometer, Thermo Scientific, ND-8000-GL).

A fragment of genomic DNA including the Exon 3 region targeted by CRISPR-Cas9 was amplified by PCR using the GoTaq G2 Green Master Mix (Promega, M7822). Two pairs of primers were used at various points: GGCATGTGGTAACAGCAG and AAGGTGTGTGCCTGTCTTC, (product size ~801bp) and GTAACAGCAGCTATTGTAGG and CAGCAGAATGGAGAGTCAC (product size ~711bp). The reaction mix was prepared by combining G2 with primers at 10μM concentration and 100ng of genomic DNA. This reaction mix was then incubated in a thermal cycler (Mastercycler X50s, Eppendorf, 6311000045) with the following parameters:

1. An initial denaturation period of 2mins at 95C
2. 40 cycles of
    a. Denaturation: 30s at 95C
    b. Annealing: 30s, increasing to the lowest melting temperature of the two primers in 5s steps of 1C
    c. Extension: 1min at 73C
3. A final extension period of 5mins at 73C

DNA gel electrophoresis was performed as follows. Gels were cast from 2% w/v agarose in tris/borate/EDTA (TBE) buffer with the addition of 0.01% SYBR Safe DNA stain (Invitrogen, S33102). Wells were loaded with 1μg of PCR product combined

with loading dye (New England Biolabs, B7025S) at 20% v/v, together with a ladder (New England Biolabs, N0551L). Gels were submerged in TBE and a potential difference of 70V was applied for approximately 2-3 hours. Gels were imaged using the iBright CL1000 Imaging System (Invitrogen, A32749).

Subclones showing a clear and bright band of a smaller amplicon size than wildtype, indicating a deletion, in gel electrophoresis were then sent for Sanger sequencing, performed using the Eurofins Genomics TubeSeq service. Samples were prepared for sequencing using the Wizard SV Gel and PCR Clean-Up System (Promega, A9281). Primers used were those used for PCR, as well as TTGGCTGTTGAAATGGCAGC and ATGTTGCAGCCATCCAGCTT (product length ~400). 15µl of PCR product at 5ng/µl was combined with 10µl of 10mM primer for sequencing.

Analysis of Gene Expression Via RT-qPCR

Total RNA was isolated from cells collected at D0 (stem cell stage), D18 (neural progenitor stage), D50 (immature neurons), and D70 (mature neurons) using either the RNeasy Mini Kit (Qiagen, 74104) or the PureLink RNA Mini Kit (Invitrogen, 12183018A). Both kits work similarly to each other, and to the earlier described DNA extraction kits. Cell membranes were lysed using a buffer containing a chaotropic agent combined with 2-mercaptoethanol, which serves as an RNase inhibitor. Cell samples were triturated with a 20-gauge needle and syringe to ensure a homogenised cell lysate. RNA was precipitated with 70% ethanol and was bound to a silica spin column membrane for washing. RNA was eluted into nuclease-free water, and RNA concentration was measured by spectrophotometry (NanoDrop™ 8000 Spectrophotometer, Thermo Scientific, ND-8000-GL).

RNA was then reverse transcribed into cDNA using the High-Capacity cDNA Reverse Transcription Kit (Applied Biosystems, 4368814). 750ng of RNA was combined with reverse transcriptase, deoxynucleoside triphosphates (dNTPs) and primers in a buffer solution. The reaction mix was then incubated in a thermal cycler (Mastercycler X50s, Eppendorf, 6311000045) with the following parameters:

1. 10mins at 25C
2. 120mins at 37C
3. 5mins at 85C

Quantitative PCR (qPCR) was performed on generated cDNA using the StepOnePlus Real-Time PCR System (Applied Biosystems, 4376600). SyGreen Blue Mix Hi-ROX (PCR Biosystems, PB20.16-20) was used, with SYBR as a fluorescent reporter and ROX as a passive normalisation dye. Primers used were from Integrated DNA Technologies and are detailed in Supplementary Figure 3. Reactions were prepared on a 96-well plate (Starlab, E1403-7700), by combining 1.5ng cDNA with SyGreen and forward and reverse primers at 10μM. qPCR reactions were run with the following parameters:

1. Hot start 2mins at 95C
2. 40 cycles of
    a. Denaturation 5s at 95C
    b. Annealing and Extension 20s at 60C

Analysis of Protein Expression by Immunoblotting

To purify protein from collected cell pellets, cells were lysed using RIPA buffer (Thermo Scientific, 89901) in the presence of a protease and phosphatase inhibitor cocktail and EDTA (Thermo Scientific, 78444). Cells were incubated in RIPA buffer for 30mins at 4C on a rotating tube mixer, after which they were centrifuged at 13000rcf for 10mins at 4C. Supernatant containing dissolved proteins was then collected and combined with LDS buffer (Invitrogen, NP0008) and a sample reducing agent containing dithiothreitol (DTT, Invitrogen, NP0009) before storing at -80C. Some supernatant was set aside for protein concentration determination via colorimetry.

Protein concentration was determined via a colorimetric Lowry-type protein assay (Bio-Rad, 5000116). 5μl of protein samples and prediluted bovine serum albumin (BSA) standards (Thermo Scientific, 23208) were combined with reagents in appropriate amounts as directed in the kit protocol on a 96-well plate. Samples and

standards were added in triplicate. The plate was agitated for 15mins on a plate rocker at RT before protein absorbance at 750nm wavelength was measured with a microplate reader (CLARIOstar Plus, BMG Labtech). Sample protein concentrations were then estimated by fitting a linear regression model of sample absorbances against known protein standard amounts and evaluating this model for measured sample absorbances.

Immunoblotting (Western blotting) was performed using sodium dodecyl sulphate-polyacrylamide gel electrophoresis (SDS-PAGE) followed by semi-dry gel transfer and antibody staining. Using predetermined protein concentrations, 40µg protein from each sample was loaded into a 1mm 4-12% precast polyacrylamide gel (Invitrogen, NW04125BOX) submerged in 1x MES running buffer (Invitrogen, NP0002). A 10-250kDa protein ladder was also loaded (New England Biolabs, P7719S). The gel was run at 75V for 20mins and then 150V for approximately 50-60mins. Gels were transferred onto a 0.2µm nitrocellulose membrane (BioRad, 1704159) using the TransBlot Turbo system (BioRad) and the membrane was then blocked with 5% skimmed milk powder in tris-buffered saline plus 0.1% Tween 20 (TBST) by agitating for 1h at RT on a plate rocker. Blotting membranes were then incubated in primary antibodies (Anti-FOXG1 antibody [EPR18987], Abcam) overnight at 4C; antibodies were placed in 5% milk in TBST at optimal concentrations as previously determined. The membrane was then washed three times with TBST before incubating in near-infrared (NIR) dye-conjugated secondary antibodies (IRDye 680, IRDye 800, LI-COR) at 0.02% concentration in 5% milk in TBST for 1hr at RT on a plate rocker. Membranes were then washed again and imaged using the Odyssey CLx Imager (LI-COR).

Data Analysis

Sanger sequencing was analysed using a sequence chromatogram viewer. Alignment to the genomic reference sequence was performed using the Clustal Omega algorithm.

RT-qPCR data was analysed in GraphPad Prism. Three biological replicates (cDNA originating from distinct cell samples) were tested per cell line and three technical

replicates were performed per cDNA sample. Modified Z-scores of C_t values of technical replicates were inspected to identify outliers within biological replicates; any replicate with a modified Z-score of greater than 3.5 was discarded as an outlier. C_t values for the reference gene (ACTB) were then averaged and this result subtracted from all other C_t values to give ΔC_t values. ΔC_t values were then transformed to relative mRNA abundances using abundance $= 2^{-\Delta C_t}$. Outlier inspection was again performed to identify outliers within conditions. Abundance values for technical replicates were then averaged within biological replicates to give a mean relative mRNA abundance for each biological replicate. Significance testing was then performed using two-way analysis of variance (ANOVA) with mean relative mRNA abundance as the dependent variable and cell line and replication as factors. Dunnett's post-hoc tests were then used to compare means of mutant cell lines with the control cell line.

Immunoblotting data was analysed by computing band signal intensity per unit area for the protein of interest and the reference protein (GAPDH). The signal intensity per unit area for the protein of interest was then divided by that of the reference protein to give a normalised signal intensity per unit area. A two-way ANOVA was then fitted with normalised signal intensity per unit area as the dependent variable and cell line and differentiation ID as factors. Dunnett's post-hoc tests were again utilised.

Results

CRISPR Stem Cell Populations Exhibit FADS2 Mutation and Corresponding Reduction in Gene Expression

Utilising initial gel electrophoresis screening, I selected two CRISPR-Cas9 stem cell populations for further genotyping, referred to as Mutant A and Mutant B. Gel electrophoresis of PCR products amplified from the Exon 3 region targeted by CRISPR indicated that both cell populations contained FADS2 mutants, with bands visible at both ~700bp (wildtype) and ~600bp (Fig 4B). Sanger sequencing of this region indicated CRISPR cut sites resulting in an approximately 114bp genomic deletion for each mutant, of which 98 base pairs were removed from Exon 3, yielding

a frameshift and consistent with gel electrophoresis results (Fig 4A). However, sequences were mixed, and this combined with gel electrophoresis results was indicative of polyclonal cell populations containing both knockout and wildtype cells.

To verify that the identified genomic mutations caused functional changes in the cell populations, I performed RT-qPCR of purified total RNA from stem cell samples of each cell population for FADS2 gene expression (Fig 4C). Samples from each of the two independent replications of differentiation used for experiments were tested. Both cell populations showed a significant reduction in FADS2 expression (Mutant B fold change 0.687, $p=0.0005$; Mutant B fold change 0.560, $p<0.0001$), as intended.

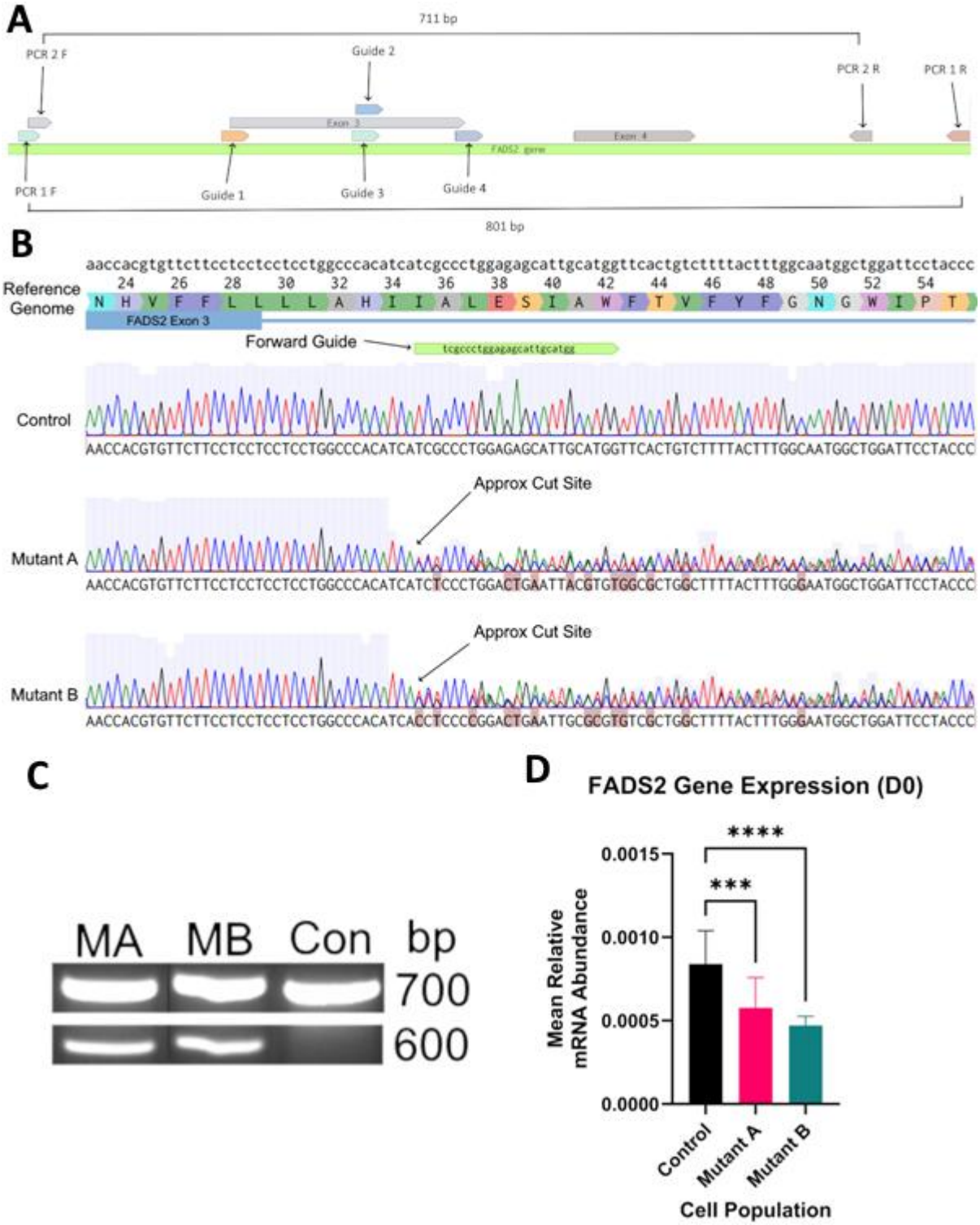

Fig 4: FADS2 Mutant Genotyping Results. (A) Schematic illustration of the CRISPR-Cas9 gene editing strategy. The four CRISPR guides, PCR primers used for genotyping, and expected product sizes are shown. (B) Sanger Sequencing representative results. Forward (shown) and reverse sequences of the region of genomic DNA targeted by CRISPR were obtained. The location of the forward CRISPR guide is shown in relation to Exon 3 of the FADS2 gene. Approximate cut sites, marked by the introduction of two competing genomic sequences and ensuing reduction in read quality, are indicated. (C) DNA gel electrophoresis

of PCR products amplified from the genomic region targeted by CRISPR. Two bands at 700bp and 600bp are clearly visible for mutant cell populations. (D) Mean relative mRNA abundances for all principal FADS2 transcripts in D0 samples as measured by RT-qPCR. Normalisation is to ACTB abundance. Significance levels are indicated (****: $p<0.0001$; ***: $p<0.001$). N=6.

FADS2 Mutants Express Normal Levels of FADS1 But Altered Levels of COX Enzymes

FADS2 is located proximally to related gene FADS1, with which it shares considerable sequence homology (Marquardt et al., 2000). To verify that the CRISPR had not produced any unintended effects on FADS1, I ran RT-qPCR for FADS1 mRNA (Fig 5A). FADS1 gene expression was found not be significantly altered from control cells. Furthermore, to preliminarily assess whether the FADS2 mutation affects expression of genes involved in downstream metabolic processes, I assessed the expression of the prostaglandin endoperoxide synthase enzymes COX1 and COX2 (PTGS1 and PTGS2) via RT-qPCR (Fig 5B-C). PTGS2 was significantly decreased in Mutant A but significantly increased in Mutant B. Similar trends were seen in PTGS1 expression, but these differences were not significant.

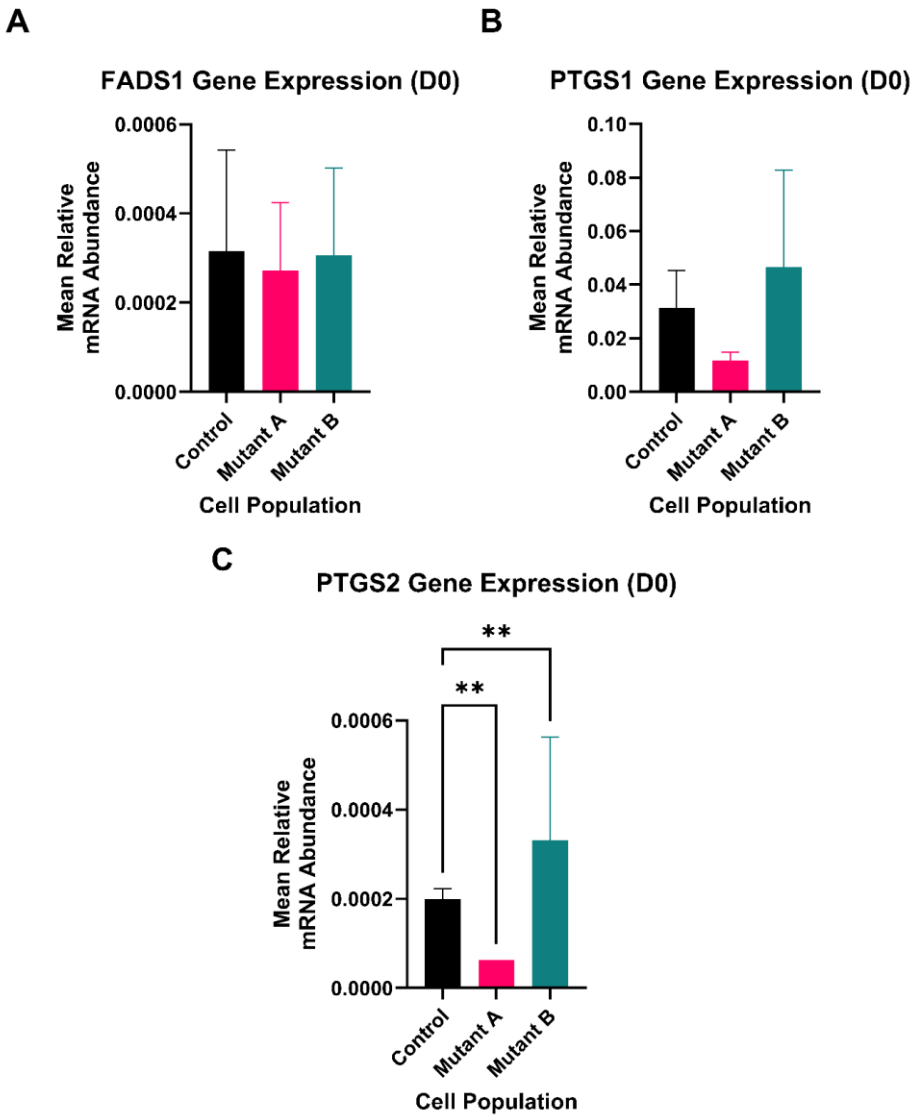

Fig 5: FADS1 and PTGS1/2 Expression (D0). All panels show mean mRNA abundances normalised to ACTB. (A) NANOG. (B) PTGS1. (C) PTGS2. Significance levels are indicated (**: $p<0.01$). N=6 for all panels.

FADS2 Mutant B Exhibits Increased NANOG Expression Compared to Control Cells

Previous literature demonstrates alterations in canonical pluripotent stem cell markers such as Oct3/4 in response to varying PUFA levels (Chang et al., 2012). To investigate any differences in the ability of FADS2 mutants to maintain a pluripotent state, I tested the expression of the well-established pluripotency markers NANOG and Oct3/4 (POU5F1), as well as the neuroectodermal lineage marker nestin (NES), at D0 via RT-qPCR (Fig 6A-C). POU5F1 and NES expression were slightly but not

significantly increased in FADS2 mutants compared to controls, however, NANOG expression in Mutant B was significantly increased (fold change 1.35, p=0.0108). The same effect was not seen in Mutant A.

Proliferation rates of human iPSCs were previously found to be increased in response to high levels of n-6 PUFAs (Dec et al., 2023), however, I hypothesised that cell growth rates would be reduced in FADS2 mutant stem cells due to reduced synthesis of all long-chain PUFAs, in line with previous literature. To assess any differences in cell proliferation in mutant cell populations compared to controls, I performed RT-qPCR for the proliferation markers MCM2, MKI56 and PCNA at D0 (Fig 6D-F. In contrast to expectations, no significant differences were observed in these markers, with some downward trends in PCNA and upward trends in MKI67.

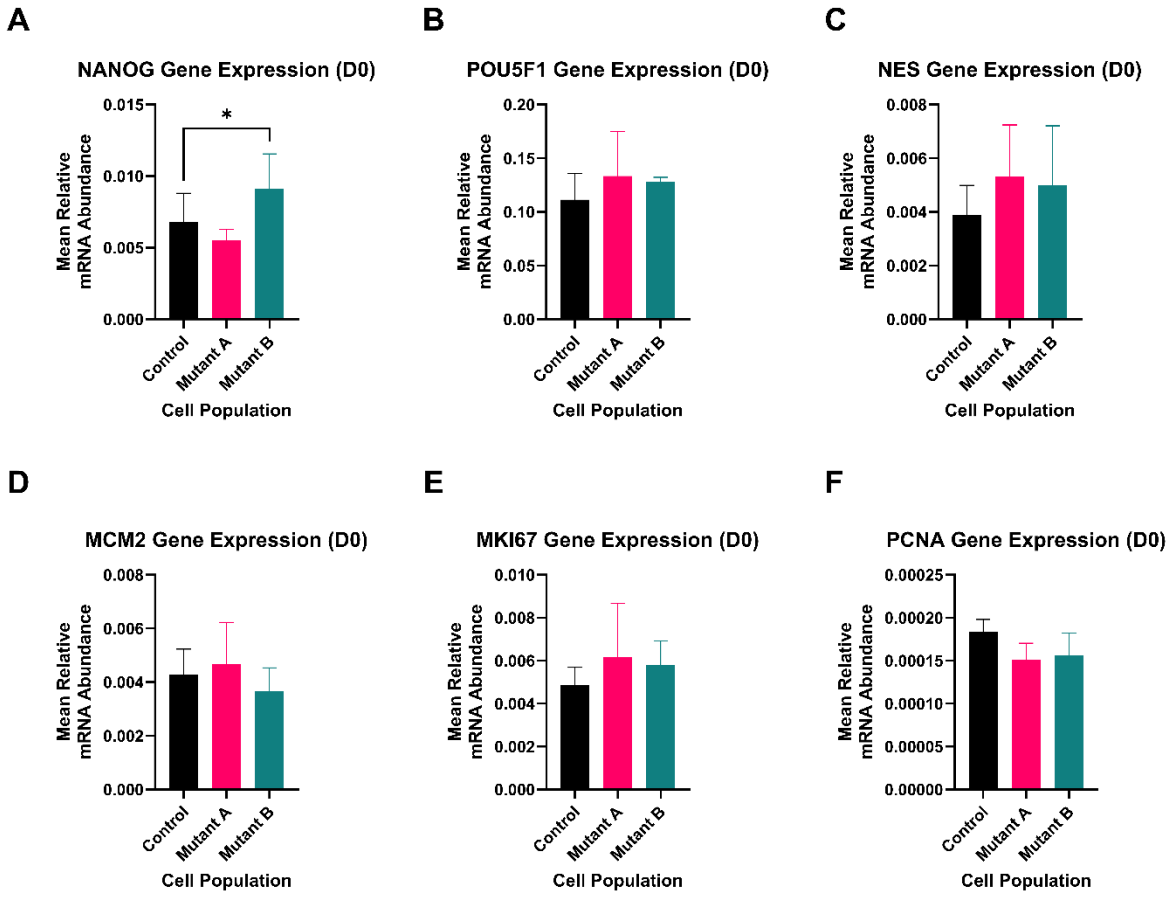

Fig 6: Stem Cell and Proliferation Marker Expression (D0). All panels show mean mRNA abundances normalised to ACTB. (A) NANOG. (B) POU5F1. (C) NES. (D) MCM2. (E) MKI67. (F) PCNA. Significance levels are indicated (*: p<0.05). N=6 for all panels.

FADS2 Mutants Show Decreased MKI67 Expression at the Neural Progenitor Stage

Previous work demonstrated that neural progenitor cells cultured in high ratios of n-6 PUFAs express lower levels of the key proliferation marker MCM2 is decreased along with that of neural progenitor cell marker NES (Dec et al., 2023). To assess the neurodevelopmental process in FADS2 mutants, I differentiated both mutants to 18-day old neural progenitor cells and assessed the expression of key genes via RT-qPCR. In these samples, I again assessed the stem cell markers NANOG and POU5F1, as well as NES (Fig 7A-C). As in stem cell samples, there was no difference in POU5F1 and NES expression at these stages, and in this case, no difference in NANOG expression was observed. However, when assessing MKI67 expression, this was found to be significantly reduced in Mutant A (Fig 7D, fold change 0.893, p=0.0353), in line with previous literature. Differences were observed between replications; in replication 1 of differentiation, both mutants exhibited significant reductions in MKI-67 expression, but these effects did not replicate in replication 2 (Fig 7E).

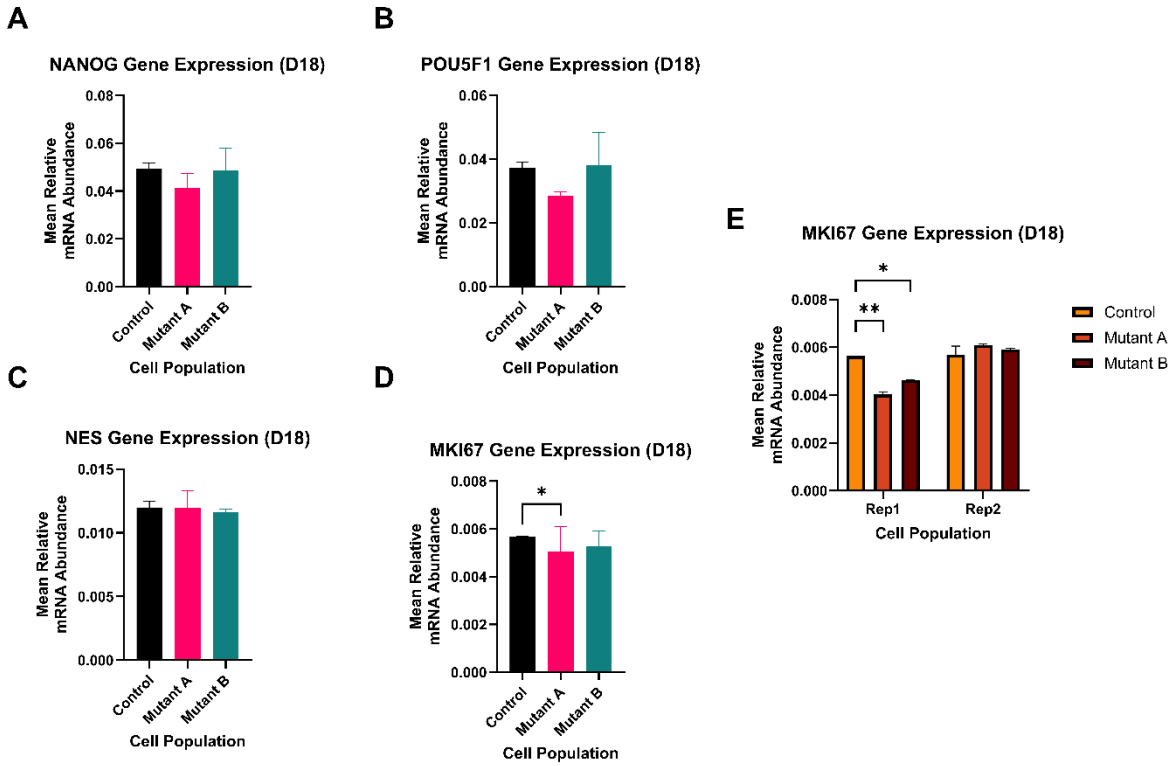

Fig 7: Stem Cell and Proliferation Marker Expression (D18). All panels show mean mRNA abundances normalised to ACTB. (A) NANOG. (B) POU5F1. (C) NES. (D) MKI67.

(E) MKI67 simple effects by replication (N=3 per effect). Significance levels are indicated (**: p<0.01; *: p<0.05). N=6 for all panels unless otherwise stated.

Gene and Protein Expression of Neural Progenitor Marker Foxg1 are Decreased in FADS2 Mutants

In addition to NES, FOXG1 is a reliable marker of the neural progenitor stage and is highly expressed at later stages prior to neuronal lineage specification (Regad et al., 2007). Owing to previous work regarding the influence of PUFA levels on FOXG1 expression (Dec et al., 2023), I tested FOXG1 expression at D18 using RT-qPCR. Overall, FOXG1 expression was slightly, but not significantly, reduced, however, in replication 1, expression was significantly reduced in both mutants (Mutant A fold change 0.643, p=0.0109; Mutant B fold change 0.686, p=0.0223; Fig 8B). This result did not replicate in replication 2. To further probe the observed difference, I performed immunoblotting for Foxg1 protein in both mutants and controls. Analysis of band signal intensities normalised to glyceraldehyde-3-phosphate dehydrogenase (Gapdh) showed a clear trend for decreased protein levels, with reduced protein levels in both mutants (Mutant A fold change 0.672, p=0.3601; Mutant B fold change 0.325, p=0.0561; Fig 8C-D). Both decreases did not reach significance.

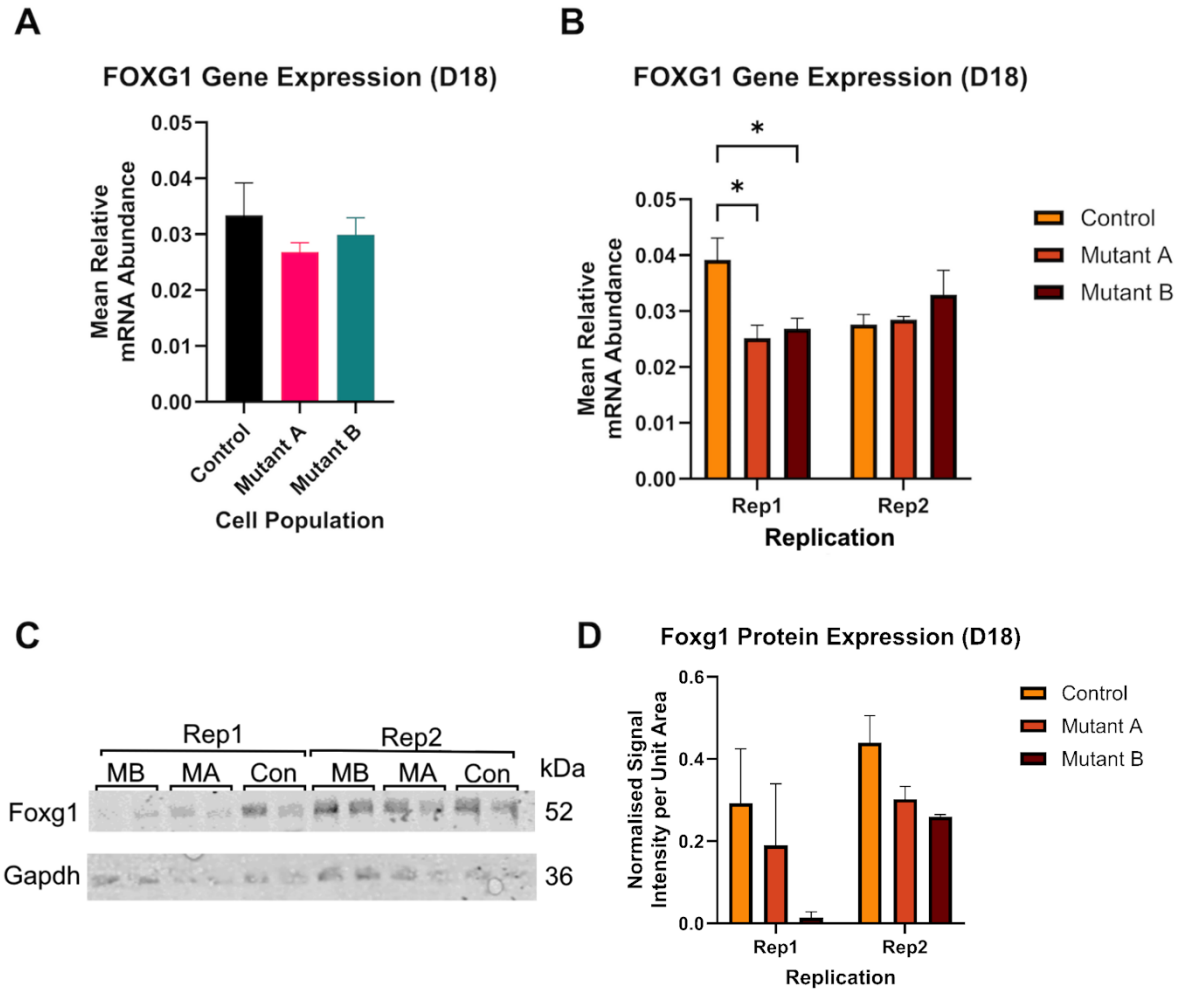

Fig 8: Foxg1 Gene and Protein Expression (D18). (A) FOXG1 mean mRNA abundance normalised to ACTB (N=6). (B) Simple effects of FOXG1 mean relative mRNA abundance by replication (N=3 per effect). (C) FOXG1 immunoblotting results. Note Mutant B is shown first. (D) Immunoblotting band signal intensity normalised to Gapdh and adjusted for band area. Significance levels are indicated where necessary (*: $p<0.05$). N=4.

FADS2 Mutant Shows a Trend Towards Decreased Generation of MAP2-Positive Cells but Increased Synaptic Marker Expression

Previous literature suggests that PUFAs regulate the generation of normal MAP2-positive neurons. To assess the generation of cortical neurons with normal gene expression patterns in the FADS2 knockout model, I analysed expression of key markers MAP2 and TUBB3 (Tuj1) at both 50- (Fig 9A-B) and 70-days (Fig 9E-F) post-induction via RT-qPCR. Due to project constraints, only three replicates were analysed at D70, as opposed to six as with other time points. No differences were observed at D50, when neurons are still immature, but at D70, MAP2 expression

showed a decreasing trend, as expected. To investigate whether these neurons were generating normal synapses, I assessed the expression levels of key synaptic markers synaptotagmin 1 (SYT1), a calcium sensor involved in exocytosis present at the presynaptic zone, and PSD95 (DLG4), a postsynaptic density component. No significant differences were detected in synaptic markers at D50 (Fig 9C-D) or D70 (Fig 9G-H), however, at D50, DLG4 was increased in the FADS2 mutant, and at D70, both SYT1 and DLG4 were upregulated, DLG4 by a factor of almost 2.5 ($p=0.0907$).

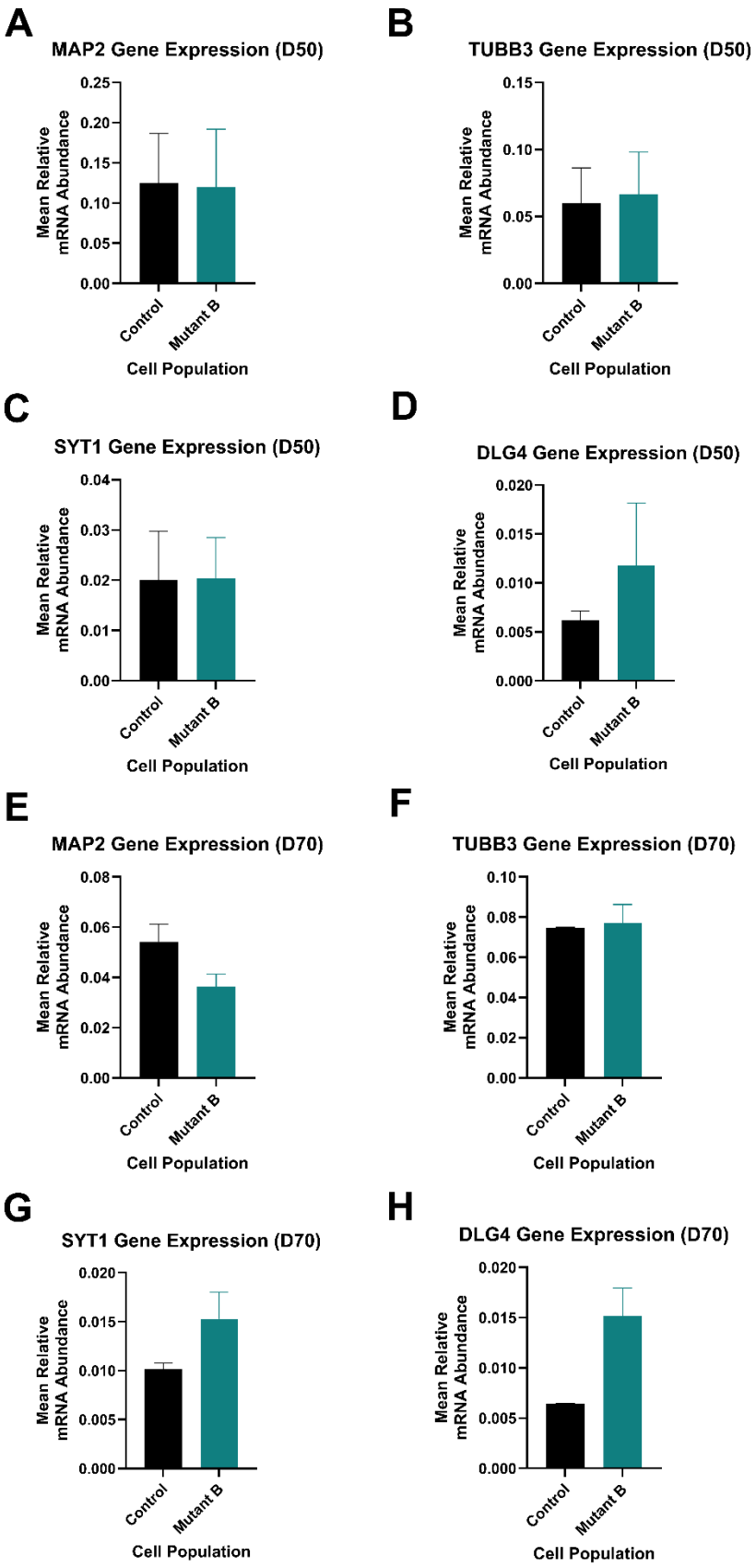

Fig 9: Neuronal and Synaptic Marker Expression (D50 and D70). All panels show mean mRNA abundances normalised to ACTB. (A) MAP2 D50. (B) TUBB3 D50. (C) SYT1 D50.

(D) DLG4 D50. (E) MAP2 D70. (F) TUBB3 D70. (G) SYT1 D70. (H) DLG4 D70. Panels A-D: N=6. Panels E-H: N=3.

Excitatory and Inhibitory Marker Expression is Altered in FADS2 Mutant Neurons at D70

Previous work showed that altered PUFA ratios disturb the balance of excitatory and inhibitory protein-encoding genes in mature neurons (Dec et al., 2023). I therefore examined the expression of glutamatergic AMPA receptor subunits 1 and 2 (GRIA1 and GRIA2), $GABA_A$ receptor subunit α1 (GABRA1), and glutamate decarboxylase 1 (GAD1/GAD67), at D50 (Fig 10A-D) and D70 (Fig 10E-H). No appreciable differences in expression were observed at D50, however, at D70, expression of GRIA1 was significantly decreased (fold change 0.453, p=0.0193) while expression of GRIA2 was significantly increased (fold change 3.95, p=0.0292). Furthermore, GABRA1 showed a trend of upregulation (fold change 2.16, p=0.1972) while GAD1 was significantly downregulated (fold change 0.516, p=0.0188).

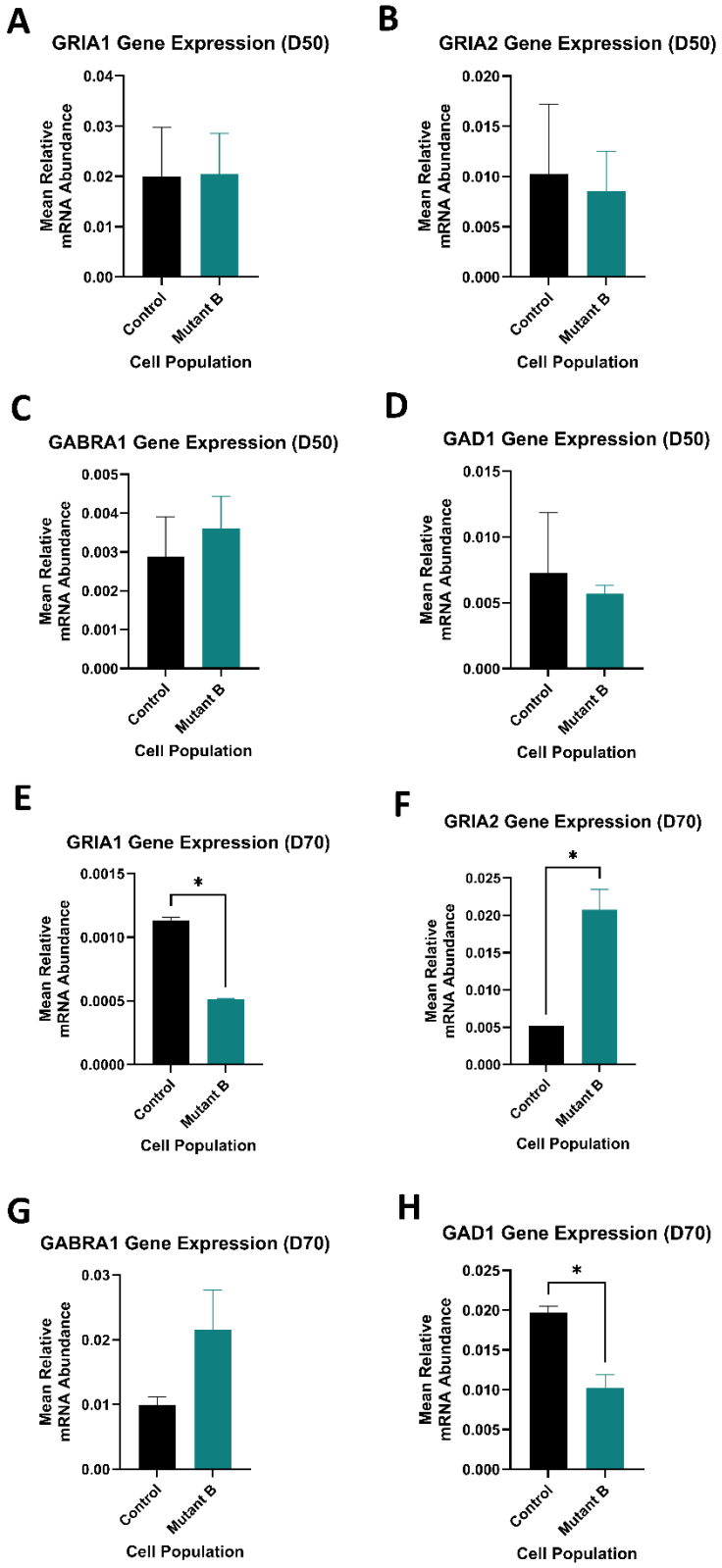

Fig 10: Excitatory and Inhibitory Marker Expression (D50 and D70). All panels show mean mRNA abundances normalised to ACTB. (A) GRIA1 D50. (B) GRIA2 D50. (C) GABRA1 D50. (D) GAD1 D50. (E) GRIA1 D70. (F) GRIA2 D70. (G) GABRA1 D70. (H) GAD1 D70. Significance levels are indicated (*: $p<0.05$). Panels A-D: N=6. Panels E-H: N=3.

Discussion

FADS2 Mutation Does Not Directly Impact Stem Cell Proliferation

Previous literature highlights the role of long-chain PUFAs in normal neurodevelopment in animal models. Here, I sought to examine the effects of a mutation in PUFA enzyme FADS2 on the *in vitro* growth of human induced pluripotent stem cells and their differentiation to cortical glutamatergic neurons. In stem cell populations, I hypothesised that the expression of key markers of proliferation would be reduced in FADS2 mutants due to the presumed decrease in mitogenic long-chain PUFAs. However, no alterations were detected in MCM2, MKI67 and PCNA expression. This result was somewhat unexpected, however, previous literature does vary with respect to n-6 and n-3 PUFAs, as well as the cell type studied. N-6-derived oxylipins have been frequently associated with agonism of mitogenic pathways such as MAPK/ERK (Krysan et al., 2005), and increased ratios of n-6:n-3 PUFAs were previously associated with decreased doubling time in iPSCs (Dec et al., 2023). On the other hand, some research indicates that n-3 PUFAs may in fact prolong the cell cycle (Wei et al., 2018). Therefore, in a FADS2 mutant model, presumably reduced levels of all long-chain PUFAs may not directly impact proliferation in stem cells, with the ratio of n-6:n-3 PUFAs perhaps being more important in this regard. Future work would benefit from performing direct *in vitro* comparisons of doubling time at multiple time points of differentiation to further ascertain how PUFAs modulate temporal aspects of cell growth and development. Considering the extensive literature regarding the anti-apoptotic effects of long-chain PUFAs, particularly n-3 PUFAs, future work should also investigate the expression of apoptotic genes in FADS2 mutants in addition to that of markers of proliferation, as cell survival may be a key phenotype in these mutants.

It is also of note that I observed a significant increase in the expression of pluripotency marker NANOG in one of the FADS2 stem cell mutant populations studied. This result is also unexpected, and since it was not replicated in both mutants, it should be treated with caution. Some previous literature exists indicating that treatment of mouse iPSCs with DHA may downregulate the expression of the key pluripotency genes Oct3/4 and c-Myc (Chang et al., 2012). Therefore, the finding

that FADS2 mutants show an opposite effect may be consistent with this, however, more investigation is certainly needed.

FOXG1 Protein Levels Are Reduced i FADS2 Mutants

Previous work done in human iPSC models found that high ratios of n-6:n-3 PUFAs in the cell culture medium during differentiation significantly reduced the expression of late-stage neural progenitor cell marker FOXG1 and demonstrated a downward trend in PAX6 (Dec et al., 2023). In the present study, I differentiated FADS2 mutant iPSCs to neural progenitor cells via dual SMAD inhibition. In agreement with previous results, a downward trend in FOXG1 gene expression was observed after 18 days of differentiation. This decrease was significant for both mutant populations in the first independent replication of experiments but did not replicate in the second repetition. It is worth noting that the fold decrease in FADS2 expression for Mutant B was of a smaller magnitude than in replication 1 (Mutant B 0.505 vs 0.649; Supplementary Figure 1). However, greatly decreased Foxg1 protein levels were observed in both mutants, with this result replicating in both repetitions of experiments. Despite the large effect sizes observed, the changes did not reach statistical significance, likely due to the use of only two samples from each independent replication leading to this preliminary assay being relatively underpowered. In addition, I found that the expression of marker of proliferation MKI67 was significantly decreased at D18 in FADS2 mutants. This is in line with previous findings that increased ratios of n-6:n-3 PUFA significantly decrease expression of MCM2 and NES at the neural progenitor stage (Dec et al., 2023).

Previous research suggests that FOXG1 expression may regulate the specification of developing neural progenitors into either glutamatergic or GABAergic neurons (e.g. Miyoshi et al., 2024). Therefore, my results raise the possibility that decreased FOXG1 protein may cause changes in excitatory and inhibitory balance in FADS2 mutant neuronal populations. Further assays including immunofluorescence would serve to examine whether FOXG1 expression is altered at the single cell level, and further replicates are necessary to confirm statistical significance. Future research should also incorporate staining for multiple additional markers of neural progenitors

such as vimentin (VIM), nestin (NES), and HES1/5 to examine whether the observed effects are specific to FOXG1 or more general.

FADS2 Mutants Exhibit A Trend Towards Reduced MAP2 Expression and Upregulated Synaptic Gene Expression at D70

In the present work, I also assessed the expression of markers of mature neurons in FADS2 mutants via measurement of MAP2 and TUBB3 gene expression. In line with previous literature in animal models (e.g. Cao et al., 2005; Kawakita et al., 2006), abnormally decreased expression of MAP2 was observed in mature D70 neurons. Such differences were not appreciable earlier in development, at D50, when neurons are more immature. The observed changes were not statistically significant, and more replicates are necessary to draw firm conclusions about the effect of FADS2 knockout on MAP2 expression in cortical cell populations. Furthermore, investigations such as immunofluorescence should be performed to identify whether individual neurons are expressing less MAP2, or less MAP2-expressing cells are being generated on a population level. Future investigations will also examine other neuronal markers including NeuN (RBFOX3).

Changes in MAP2 expression were accompanied by large but non-significant increases in genes encoding both key presynaptic and postsynaptic proteins. The influence of PUFAs on synaptic processes, such as vesicle release and recycling, is well documented, and previous literature demonstrated small increases in SNAP25, SYP and DLG4 expression in response to altered ratios of n-6 to n-3 PUFAs in culture medium in an iPSC-derived model (Dec et al., 2023). However, the increases in synaptic gene expression observed here are of a much a larger magnitude than seen previously. Long-chain PUFA-derived phosphoinositides are key for the regulation of synaptic vesicle dynamics (Posor et al., 2022), and I suggest that presumed decreases in long-chain PUFAs in FADS2 mutants may impair the ability of exocytic and endocytic proteins to correctly localise to phosphoinositides. In this vane, it may be the case that the observed increases in synaptic gene expression may represent a compensatory mechanism for abnormal synaptic function, and I suggest that both synaptogenesis and vesicle dynamics represent promising areas for future research in PUFA models. Initial follow-up experiments should focus on

validating the observed effects at the single cell level with immunofluorescence and should examine protein levels by immunoblotting.

Excitatory and Inhibitory Marker Expression is Altered in FADS2 Mutant Neurons

Previous work found that PUFA ratios influence glutamatergic neuronal activity as measured by multielectrode array electrophysiology *in vivo* (Dec et al., 2023). This was accompanied by the finding that expression of GABA receptor subunits GABRA1, GABRA2, and GABRB1 was significantly increased, with a corresponding upward trend in glutamate decarboxylase GAD1. Expression of AMPA receptor subunits GRIA1 and GRIA2 was also slightly increased, though not significantly. To probe such differences in FADS2 mutants, I measured expression of GABRA1 and GAD1, and GRIA1 and GRIA2, respectively taken as indicators of inhibitory and excitatory tendency. Expression levels were unaltered in immature neurons at D50, but at D70, large and opposing differences were observed, with a significant decrease in GRIA1 but a significant increase in GRIA2, and a significant increase in GABRA1 but a significant decrease in GAD1.

I had hypothesised that both GRIA1 and GRIA2 would be decreased, however, previous literature reports that altered expression of individual subunits may be associated with neuropsychiatric conditions such as schizophrenia (O'Connor and Hemby, 2007). Varying synaptic expression of AMPA receptors plays a key role in both long-term potentiation (LTP) and depression (LTD) (Kessels and Malinow, 2009), and there is evidence that disruption of the expression of individual receptor subunits such as GRIA2 may cause detrimental phenotypes including altered synaptic plasticity (Isaac et al., 2007). The opposite changes in GRIA1 and GRIA2 expression observed may represent a compensatory mechanism. Similarly, previous literature reports that changes in GABA receptor expression can occur independently of changes in GAD expression in a neuropsychiatric model (Raud et al., 2009). Again, this may represent a homeostatic mechanism.

Taken together, these results present preliminary evidence that altered PUFA metabolism may affect the expression of excitatory and inhibitory markers in

neuronal populations. To investigate whether such changes translate to altered excitatory/inhibitory balance in network dynamics as previously observed, future research should perform functional assays such as *in vitro* electrophysiological analysis of FADS2 mutant neurons using multielectrode arrays. Furthermore, greater accumulation of molecular evidence such as immunofluorescence and immunoblotting is necessary to strengthen the observed effects.

Limitations of the Present Study

A limitation of the present study is that experiments were conducted with polyclonal cell populations consisting of both mutant and wildtype cells. A consequence of the presence of wildtype cells in each cell population is that observed phenotypes may be masked or confounded, complicating interpretation of results. Future work will necessitate the isolation of monoclonal FADS2 knockout populations to ensure robust phenotypes and may benefit from the comparison of both homozygous and heterozygous FADS2 mutant cells with wildtype cells, as previous literature found that a heterozygous, but not homozygous, FADS2 deletion presented a robust behavioural model of bipolar disorder in mice (Yamamoto et al., 2023).

A major limitation of the work presented here is its reliance on RT-qPCR data to probe neurodevelopmental markers in the cell populations of interest. RT-qPCR is sensitive at the population level but does not provide information about individual cells, protein levels, or localisation. Conclusions about changing cell types within the cell populations assessed, such as a switch from excitatory to inhibitory lineages, cannot therefore be drawn at this stage. Future work must incorporate additional assays such as immunofluorescence to further strengthen the results presented here.

Another important point to consider is that, because the presented FADS2 knockout is a stable, long-term perturbation, the effects observed in this model may be confounded by compensatory metabolic changes rather than only the direct biochemical effects of impaired Δ6-desaturation. For example, cells may adjust PUFA uptake, elongation and transport to attempt to maintain homeostasis, meaning that the observed phenotype represents both the loss of FADS2 activity and the

adaptive responses triggered by that loss. Future studies should always be aware of this when interpreting results.

Conclusions

Taken together, the results presented here lend tentative support to the notion that altered early neurodevelopment is a promising area of dysfunction to investigate in models of altered long-chain PUFA metabolism. Increased FOXG1 expression has previously been implicated in abnormal increases in the generation of GABAergic neurons in telencephalic organoids derived from autism spectrum disorder (ASD) patient iPSCs (Mariani et al., 2015), and polymorphisms in FADS2 are associated with bipolar risk (e.g. Mullins et al., 2021). Therefore, future investigation of FOXG1 dysregulation in altered PUFA models has relevance to neurodevelopmental and neuropsychiatric disease pathophysiology. Moreover, the preliminary finding that FADS2 mutants exhibit altered expression of excitatory and inhibitory markers merits further investigation, with altered GABAergic development previously associated with schizophrenia (Schmidt and Mirnics, 2015), autism (Uzunova et al., 2016), and bipolar disorder (Hu et al., 2023). Future work in FADS2 mutants and models of altered long-chain PUFA metabolism will serve to reinforce early findings and work towards identifying potential mechanisms and possible drug targets.

References

Ashizawa, T. et al. 2024. Association of plasma arachidonic acid levels with a bipolar disorder and the effects of a FADS gene variant. *Translational Psychiatry* 14(1), p. 435. doi: 10.1038/s41398-024-03141-1.

Baccouch, R. et al. 2023. The impact of lipid polyunsaturation on the physical and mechanical properties of lipid membranes. *Biochimica et Biophysica Acta (BBA) - Biomembranes* 1865(2), p. 184084. doi: 10.1016/j.bbamem.2022.184084.

Bae, S.-K., Bessho, Y., Hojo, M. and Kageyama, R. 2000. The bHLH gene *Hes6* , an inhibitor of *Hes1* , promotes neuronal differentiation. *Development* 127(13), pp. 2933–2943. doi: 10.1242/dev.127.13.2933.

Basil, M.C. and Levy, B.D. 2016. Specialized pro-resolving mediators: endogenous regulators of infection and inflammation. *Nature Reviews Immunology* 16(1), pp. 51–67. doi: 10.1038/nri.2015.4.

Bazinet, R.P. and Layé, S. 2014. Polyunsaturated fatty acids and their metabolites in brain function and disease. *Nature Reviews Neuroscience* 15(12), pp. 771–785. doi: 10.1038/nrn3820.

Beltz, B.S., Tlusty, M.F., Benton, J.L. and Sandeman, D.C. 2007. Omega-3 fatty acids upregulate adult neurogenesis. *Neuroscience Letters* 415(2), pp. 154–158. doi: 10.1016/j.neulet.2007.01.010.

Ben Gedalya, T., Loeb, V., Israeli, E., Altschuler, Y., Selkoe, D.J. and Sharon, R. 2009. α-Synuclein and Polyunsaturated Fatty Acids Promote Clathrin-Mediated Endocytosis and Synaptic Vesicle Recycling. *Traffic* 10(2), pp. 218–234. doi: 10.1111/j.1600-0854.2008.00853.x.

Bhat, K.M.R. 2006. Transcriptional regulation of human MAP2 gene in melanoma: role of neuronal bHLH factors and Notch1 signaling. *Nucleic Acids Research* 34(13), pp. 3819–3832. doi: 10.1093/nar/gkl476.

Boergermann, J.H., Kopf, J., Yu, P.B. and Knaus, P. 2010. Dorsomorphin and LDN-193189 inhibit BMP-mediated Smad, p38 and Akt signalling in C2C12 cells. *The International Journal of Biochemistry & Cell Biology* 42(11), pp. 1802–1807. doi: 10.1016/j.biocel.2010.07.018.

Brenner, R.R. 2003. Hormonal modulation of Δ6 and Δ5 desaturases: case of diabetes. *Prostaglandins, Leukotrienes and Essential Fatty Acids* 68(2), pp. 151–162. doi: 10.1016/S0952-3278(02)00265-X.

Calder, P. and Grimble, R. 2002. Polyunsaturated fatty acids, inflammation and immunity. *European Journal of Clinical Nutrition* 56(S3), pp. S14–S19. doi: 10.1038/sj.ejcn.1601478.

Calder, P.C. 2012. Mechanisms of Action of (n-3) Fatty Acids,. *The Journal of Nutrition* 142(3), pp. 592S-599S. doi: 10.3945/jn.111.155259.

Calder, P.C. 2020. Eicosanoids. Harwood, J. and Lloyd-Evans, E. eds. *Essays in Biochemistry* 64(3), pp. 423–441. doi: 10.1042/EBC20190083.

Cao, D., Xue, R., Xu, J. and Liu, Z. 2005. Effects of docosahexaenoic acid on the survival and neurite outgrowth of rat cortical neurons in primary cultures. *The Journal of Nutritional Biochemistry* 16(9), pp. 538–546. doi: 10.1016/j.jnutbio.2005.02.002.

Castillo, P.E., Younts, T.J., Chávez, A.E. and Hashimotodani, Y. 2012. Endocannabinoid Signaling and Synaptic Function. *Neuron* 76(1), pp. 70–81. doi: 10.1016/j.neuron.2012.09.020.

Ceccarini, M.R. et al. 2022. The Polyunsaturated Fatty Acid EPA, but Not DHA, Enhances Neurotrophic Factor Expression through Epigenetic Mechanisms and Protects against Parkinsonian Neuronal Cell Death. *International Journal of Molecular Sciences* 23(24), p. 16176. doi: 10.3390/ijms232416176.

Chang, Y.-L. et al. 2012. Docosahexaenoic Acid Promotes Dopaminergic Differentiation in Induced Pluripotent Stem Cells and Inhibits Teratoma Formation in Rats with Parkinson-Like Pathology. *Cell Transplantation* 21(1), pp. 313–332. doi: 10.3727/096368911X580572.

Chen, J., Fujii, K., Zhang, L., Roberts, T. and Fu, H. 2001. Raf-1 promotes cell survival by antagonizing apoptosis signal-regulating kinase 1 through a MEK–ERK independent mechanism. *Proceedings of the National Academy of Sciences* 98(14), pp. 7783–7788. doi: 10.1073/pnas.141224398.

Chen, X. et al. 2018. Omega-3 polyunsaturated fatty acid attenuates traumatic brain injury-induced neuronal apoptosis by inducing autophagy through the upregulation of SIRT1-mediated deacetylation of Beclin-1. *Journal of Neuroinflammation* 15(1), p. 310. doi: 10.1186/s12974-018-1345-8.

Chiu, C.-C., Huang, S.-Y., Su, K.-P., Lu, M.-L., Huang, M.-C., Chen, C.-C. and Shen, W.W. 2003. Polyunsaturated fatty acid deficit in patients with bipolar mania. *European Neuropsychopharmacology* 13(2), pp. 99–103. doi: 10.1016/S0924-977X(02)00130-X.

Cordain, L. et al. 2005. Origins and evolution of the Western diet: health implications for the 21st century1,2. *The American Journal of Clinical Nutrition* 81(2), pp. 341–354. doi: 10.1093/ajcn.81.2.341.

Dec, K., Alsaqati, M., Morgan, J., Deshpande, S., Wood, J., Hall, J. and Harwood, A.J. 2023. A high ratio of linoleic acid (n-6 PUFA) to alpha-linolenic acid (n-3 PUFA) adversely affects early stage of human neuronal differentiation and electrophysiological activity of glutamatergic neurons in vitro. *Frontiers in Cell and Developmental Biology* 11, p. 1166808. doi: 10.3389/fcell.2023.1166808.

Decressac, M., Volakakis, N., Björklund, A. and Perlmann, T. 2013. NURR1 in Parkinson disease—from pathogenesis to therapeutic potential. *Nature Reviews Neurology* 9(11), pp. 629–636. doi: 10.1038/nrneurol.2013.209.

Dong, Y., Xu, M., Kalueff, A.V. and Song, C. 2018. Dietary eicosapentaenoic acid normalizes hippocampal omega-3 and 6 polyunsaturated fatty acid profile, attenuates glial activation and regulates BDNF function in a rodent model of neuroinflammation induced by central interleukin-1β administration. *European Journal of Nutrition* 57(5), pp. 1781–1791. doi: 10.1007/s00394-017-1462-7.

Duan, W., Zhang, Y.-P., Hou, Z., Huang, C., Zhu, H., Zhang, C.-Q. and Yin, Q. 2016. Novel Insights into NeuN: from Neuronal Marker to Splicing Regulator. *Molecular Neurobiology* 53(3), pp. 1637–1647. doi: 10.1007/s12035-015-9122-5.

Echeverría, F., Ortiz, M., Valenzuela, R. and Videla, L.A. 2016. Long-chain polyunsaturated fatty acids regulation of PPARs, signaling: Relationship to tissue development and aging. *Prostaglandins, Leukotrienes and Essential Fatty Acids* 114, pp. 28–34. doi: 10.1016/j.plefa.2016.10.001.

Fujino, H., West, K.A. and Regan, J.W. 2002. Phosphorylation of Glycogen Synthase Kinase-3 and Stimulation of T-cell Factor Signaling following Activation of EP2 and EP4 Prostanoid Receptors by Prostaglandin E2. *Journal of Biological Chemistry* 277(4), pp. 2614–2619. doi: 10.1074/jbc.M109440200.

He, C., Qu, X., Cui, L., Wang, J. and Kang, J.X. 2009. Improved spatial learning performance of fat-1 mice is associated with enhanced neurogenesis and neuritogenesis by docosahexaenoic acid. *Proceedings of the National Academy of Sciences* 106(27), pp. 11370–11375. doi: 10.1073/pnas.0904835106.

Hoen, W.P., Lijmer, J.G., Duran, M., Wanders, R.J.A., Van Beveren, N.J.M. and De Haan, L. 2013. Red blood cell polyunsaturated fatty acids measured in red blood cells and schizophrenia: A meta-analysis. *Psychiatry Research* 207(1–2), pp. 1–12. doi: 10.1016/j.psychres.2012.09.041.

Horrobin, D. 1993. Fatty acid metabolism in health and disease: the role of Δ-6-desaturase. *The American Journal of Clinical Nutrition* 57(5), pp. 732S-737S. doi: 10.1093/ajcn/57.5.732S.

Hu, Y.-T., Tan, Z.-L., Hirjak, D. and Northoff, G. 2023. Brain-wide changes in excitation-inhibition balance of major depressive disorder: a systematic review of topographic patterns of GABA- and glutamatergic alterations. *Molecular Psychiatry* 28(8), pp. 3257–3266. doi: 10.1038/s41380-023-02193-x.

Igarashi, M., Ma, K., Gao, F., Kim, H.-W., Greenstein, D., Rapoport, S.I. and Rao, J.S. 2010. Brain lipid concentrations in bipolar disorder. *Journal of Psychiatric Research* 44(3), pp. 177–182. doi: 10.1016/j.jpsychires.2009.08.001.

Ikeda, M. et al. 2018. A genome-wide association study identifies two novel susceptibility loci and trans population polygenicity associated with bipolar disorder. *Molecular Psychiatry* 23(3), pp. 639–647. doi: 10.1038/mp.2016.259.

Inman, G.J. et al. 2002. SB-431542 Is a Potent and Specific Inhibitor of Transforming Growth Factor-β Superfamily Type I Activin Receptor-Like Kinase (ALK) Receptors ALK4, ALK5, and ALK7. *Molecular Pharmacology* 62(1), pp. 65–74. doi: 10.1124/mol.62.1.65.

Inoue, T. et al. 2017. Omega-3 polyunsaturated fatty acids suppress the inflammatory responses of lipopolysaccharide-stimulated mouse microglia by activating SIRT1 pathways. *Biochimica et Biophysica Acta (BBA) - Molecular and Cell Biology of Lipids* 1862(5), pp. 552–560. doi: 10.1016/j.bbalip.2017.02.010.

Irving, C.B., Mumby-Croft, R. and Joy, L.A. 2006. Polyunsaturated fatty acid supplementation for schizophrenia. Cochrane Schizophrenia Group ed. *Cochrane Database of Systematic Reviews*. Available at: https://doi.wiley.com/10.1002/14651858.CD001257.pub2 [Accessed: 26 November 2024].

Isaac, J.T.R., Ashby, M.C. and McBain, C.J. 2007. The Role of the GluR2 Subunit in AMPA Receptor Function and Synaptic Plasticity. *Neuron* 54(6), pp. 859–871. doi: 10.1016/j.neuron.2007.06.001.

Ishizaki, T., Uehata, M., Tamechika, I., Keel, J., Nonomura, K., Maekawa, M. and Narumiya, S. 2000. Pharmacological properties of Y-27632, a specific inhibitor of rho-associated kinases. *Molecular Pharmacology* 57(5), pp. 976–983.

Jacobs, M.L., Faizi, H.A., Peruzzi, J.A., Vlahovska, P.M. and Kamat, N.P. 2021. EPA and DHA differentially modulate membrane elasticity in the presence of cholesterol. *Biophysical Journal* 120(11), pp. 2317–2329. doi: 10.1016/j.bpj.2021.04.009.

Jones, H.J. et al. 2021. Associations between plasma fatty acid concentrations and schizophrenia: a two-sample Mendelian randomisation study. *The Lancet Psychiatry* 8(12), pp. 1062–1070. doi: 10.1016/S2215-0366(21)00286-8.

Kang, J.X., Wang, J., Wu, L. and Kang, Z.B. 2004. Fat-1 mice convert n-6 to n-3 fatty acids. *Nature* 427(6974), pp. 504–504. doi: 10.1038/427504a.

Kang, R., Zeh, H.J., Lotze, M.T. and Tang, D. 2011. The Beclin 1 network regulates autophagy and apoptosis. *Cell Death & Differentiation* 18(4), pp. 571–580. doi: 10.1038/cdd.2010.191.

Katakura, M., Hashimoto, M., Okui, T., Shahdat, H.M., Matsuzaki, K. and Shido, O. 2013. Omega-3 Polyunsaturated Fatty Acids Enhance Neuronal Differentiation in Cultured Rat Neural Stem Cells. *Stem Cells International* 2013, pp. 1–9. doi: 10.1155/2013/490476.

Katakura, M., Hashimoto, M., Shahdat, H.M., Gamoh, S., Okui, T., Matsuzaki, K. and Shido, O. 2009. Docosahexaenoic acid promotes neuronal differentiation by regulating basic helix–loop–helix transcription factors and cell cycle in neural stem cells. *Neuroscience* 160(3), pp. 651–660. doi: 10.1016/j.neuroscience.2009.02.057.

Kawakita, E., Hashimoto, M. and Shido, O. 2006. Docosahexaenoic acid promotes neurogenesis in vitro and in vivo. *Neuroscience* 139(3), pp. 991–997. doi: 10.1016/j.neuroscience.2006.01.021.

Kelly, L. et al. 2011. The polyunsaturated fatty acids, EPA and DPA exert a protective effect in the hippocampus of the aged rat. *Neurobiology of Aging* 32(12), p. 2318.e1-2318.e15. doi: 10.1016/j.neurobiolaging.2010.04.001.

Kessels, H.W. and Malinow, R. 2009. Synaptic AMPA Receptor Plasticity and Behavior. *Neuron* 61(3), pp. 340–350. doi: 10.1016/j.neuron.2009.01.015.

Kim, H., Akbar, M. and Lau, A. 2003. Effects of docosapentaenoic acid on neuronal apoptosis. *Lipids* 38(4), pp. 453–457. doi: 10.1007/s11745-003-1083-z.

Kim, H.-Y., Akbar, M. and Kim, Y.-S. 2010. Phosphatidylserine-dependent neuroprotective signaling promoted by docosahexaenoic acid. *Prostaglandins, Leukotrienes and Essential Fatty Acids (PLEFA)* 82(4–6), pp. 165–172. doi: 10.1016/j.plefa.2010.02.025.

Koga, N. et al. 2019. Altered polyunsaturated fatty acid levels in relation to proinflammatory cytokines, fatty acid desaturase genotype, and diet in bipolar disorder. *Translational Psychiatry* 9(1), p. 208. doi: 10.1038/s41398-019-0536-0.

Kou, W., Luchtman, D. and Song, C. 2008. Eicosapentaenoic acid (EPA) increases cell viability and expression of neurotrophin receptors in retinoic acid and brain-derived neurotrophic factor differentiated SH-SY5Y cells. *European Journal of Nutrition* 47(2), pp. 104–113. doi: 10.1007/s00394-008-0703-1.

Krysan, K., Reckamp, K.L., Dalwadi, H., Sharma, S., Rozengurt, E., Dohadwala, M. and Dubinett, S.M. 2005. Prostaglandin E2 Activates Mitogen-Activated Protein Kinase/Erk Pathway Signaling and Cell Proliferation in Non–Small Cell Lung Cancer Cells in an Epidermal Growth Factor Receptor–Independent Manner. *Cancer Research* 65(14), pp. 6275–6281. doi: 10.1158/0008-5472.CAN-05-0216.

Lafourcade, M. et al. 2011. Nutritional omega-3 deficiency abolishes endocannabinoid-mediated neuronal functions. *Nature Neuroscience* 14(3), pp. 345–350. doi: 10.1038/nn.2736.

Larrieu, T., Madore, C., Joffre, C. and Layé, S. 2012. Nutritional n-3 polyunsaturated fatty acids deficiency alters cannabinoid receptor signaling pathway in the brain and associated anxiety-like behavior in mice. *Journal of Physiology and Biochemistry* 68(4), pp. 671–681. doi: 10.1007/s13105-012-0179-6.

Latham, C.F., Osborne, S.L., Cryle, M.J. and Meunier, F.A. 2007. Arachidonic acid potentiates exocytosis and allows neuronal SNARE complex to interact with Munc18a. *Journal of Neurochemistry* 100(6), pp. 1543–1554. doi: 10.1111/j.1471-4159.2006.04286.x.

Lee, J., Lee, H., Kang, S. and Park, W. 2016. Fatty Acid Desaturases, Polyunsaturated Fatty Acid Regulation, and Biotechnological Advances. *Nutrients* 8(1), p. 23. doi: 10.3390/nu8010023.

Levental, K.R. et al. 2017. ω-3 polyunsaturated fatty acids direct differentiation of the membrane phenotype in mesenchymal stem cells to potentiate osteogenesis. *Science Advances* 3(11), p. eaao1193. doi: 10.1126/sciadv.aao1193.

Li, Y. et al. 2018. PPAR-γ and Wnt Regulate the Differentiation of MSCs into Adipocytes and Osteoblasts Respectively. *Current Stem Cell Research & Therapy* 13(3), pp. 185–192. doi: 10.2174/1574888X12666171012141908.

Liu, Q. et al. 2014. Omega-3 Polyunsaturated Fatty Acids Protect Neural Progenitor Cells against Oxidative Injury. *Marine Drugs* 12(5), pp. 2341–2356. doi: 10.3390/md12052341.

Lukiw, W.J. et al. 2005. A role for docosahexaenoic acid-derived neuroprotectin D1 in neural cell survival and Alzheimer disease. *The Journal of Clinical Investigation* 115(10), pp. 2774–2783. doi: 10.1172/JCI25420.

Ma, Q. 2013. Role of Nrf2 in Oxidative Stress and Toxicity. *Annual Review of Pharmacology and Toxicology* 53(1), pp. 401–426. doi: 10.1146/annurev-pharmtox-011112-140320.

Maekawa, M. et al. 2009. Arachidonic Acid Drives Postnatal Neurogenesis and Elicits a Beneficial Effect on Prepulse Inhibition, a Biological Trait of Psychiatric Illnesses. Hashimoto, K. ed. *PLoS ONE* 4(4), p. e5085. doi: 10.1371/journal.pone.0005085.

Mariani, J. et al. 2015. FOXG1-Dependent Dysregulation of GABA/Glutamate Neuron Differentiation in Autism Spectrum Disorders. *Cell* 162(2), pp. 375–390. doi: 10.1016/j.cell.2015.06.034.

Marquardt, A., Stöhr, H., White, K. and Weber, B.H.F. 2000. cDNA Cloning, Genomic Structure, and Chromosomal Localization of Three Members of the Human Fatty Acid Desaturase Family. *Genomics* 66(2), pp. 175–183. doi: 10.1006/geno.2000.6196.

McNamara, R.K., Jandacek, R., Rider, T., Tso, P., Stanford, K.E., Hahn, C.-G. and Richtand, N.M. 2008. Deficits in docosahexaenoic acid and associated elevations in the metabolism of arachidonic acid and saturated fatty acids in the postmortem orbitofrontal cortex of patients with bipolar disorder. *Psychiatry Research* 160(3), pp. 285–299. doi: 10.1016/j.psychres.2007.08.021.

McNamara, R.K. and Welge, J.A. 2016. Meta-analysis of erythrocyte polyunsaturated fatty acid biostatus in bipolar disorder. *Bipolar Disorders* 18(3), pp. 300–306. doi: 10.1111/bdi.12386.

Menezes, J. and Luskin, M. 1994. Expression of neuron-specific tubulin defines a novel population in the proliferative layers of the developing telencephalon. *The Journal of Neuroscience* 14(9), pp. 5399–5416. doi: 10.1523/JNEUROSCI.14-09-05399.1994.

Miyoshi, G., Ueta, Y., Yagasaki, Y., Kishi, Y., Fishell, G., Machold, R.P. and Miyata, M. 2024. Developmental trajectories of GABAergic cortical interneurons are sequentially modulated by dynamic FoxG1 expression levels. Proceedings of the National Academy of Sciences 121(16), p. e2317783121. doi: 10.1073/pnas.2317783121.

Mukherjee, P.K., Marcheselli, V.L., Serhan, C.N. and Bazan, N.G. 2004. Neuroprotectin D1: A docosahexaenoic acid-derived docosatriene protects human retinal pigment epithelial cells from oxidative stress. *Proceedings of the National Academy of Sciences* 101(22), pp. 8491–8496. doi: 10.1073/pnas.0402531101.

Mullins, N. et al. 2021. Genome-wide association study of more than 40,000 bipolar disorder cases provides new insights into the underlying biology. *Nature Genetics* 53(6), pp. 817–829. doi: 10.1038/s41588-021-00857-4.

O'Connor, J.A. and Hemby, S.E. 2007. Elevated GRIA1 mRNA expression in Layer II/III and V pyramidal cells of the DLPFC in schizophrenia. *Schizophrenia Research* 97(1–3), pp. 277–288. doi: 10.1016/j.schres.2007.09.022.

Orr, S.K. et al. 2013. Unesterified docosahexaenoic acid is protective in neuroinflammation. *Journal of Neurochemistry* 127(3), pp. 378–393. doi: 10.1111/jnc.12392.

Park, H. and Poo, M. 2013. Neurotrophin regulation of neural circuit development and function. *Nature Reviews Neuroscience* 14(1), pp. 7–23. doi: 10.1038/nrn3379.

Pinot, M. et al. 2014. Polyunsaturated phospholipids facilitate membrane deformation and fission by endocytic proteins. *Science* 345(6197), pp. 693–697. doi: 10.1126/science.1255288.

Posor, Y., Jang, W. and Haucke, V. 2022. Phosphoinositides as membrane organizers. *Nature Reviews Molecular Cell Biology* 23(12), pp. 797–816. doi: 10.1038/s41580-022-00490-x.

Rabehl, M. et al. 2024. Effect of FADS1 SNPs rs174546, rs174547 and rs174550 on blood fatty acid profiles and plasma free oxylipins. *Frontiers in Nutrition* 11, p. 1356986. doi: 10.3389/fnut.2024.1356986.

Raud, S., Sütt, S., Luuk, H., Plaas, M., Innos, J., Kõks, S. and Vasar, E. 2009. Relation between increased anxiety and reduced expression of alpha1 and alpha2 subunits of GABAA receptors in Wfs1-deficient mice. *Neuroscience Letters* 460(2), pp. 138–142. doi: 10.1016/j.neulet.2009.05.054.

Regad, T., Roth, M., Bredenkamp, N., Illing, N. and Papalopulu, N. 2007. The neural progenitor-specifying activity of FoxG1 is antagonistically regulated by CKI and FGF. *Nature Cell Biology* 9(5), pp. 531–540. doi: 10.1038/ncb1573.

Remy, I., Montmarquette, A. and Michnick, S.W. 2004. PKB/Akt modulates TGF-β signalling through a direct interaction with Smad3. *Nature Cell Biology* 6(4), pp. 358–365. doi: 10.1038/ncb1113.

Romanauska, A. and Köhler, A. 2023. Lipid saturation controls nuclear envelope function. *Nature Cell Biology* 25(9), pp. 1290–1302. doi: 10.1038/s41556-023-01207-8.

Sakayori, N., Maekawa, M., Numayama-Tsuruta, K., Katura, T., Moriya, T. and Osumi, N. 2011. Distinctive effects of arachidonic acid and docosahexaenoic acid on neural stem /progenitor cells: Fatty acids in neurogenesis in vitro. *Genes to Cells* 16(7), pp. 778–790. doi: 10.1111/j.1365-2443.2011.01527.x.

Schmidt, M.J. and Mirnics, K. 2015. Neurodevelopment, GABA System Dysfunction, and Schizophrenia. *Neuropsychopharmacology* 40(1), pp. 190–206. doi: 10.1038/npp.2014.95.

Schmitz, G. and Ecker, J. 2008. The opposing effects of n−3 and n−6 fatty acids. *Progress in Lipid Research* 47(2), pp. 147–155. doi: 10.1016/j.plipres.2007.12.004.

Shi, Y., Kirwan, P. and Livesey, F.J. 2012. Directed differentiation of human pluripotent stem cells to cerebral cortex neurons and neural networks. *Nature Protocols* 7(10), pp. 1836–1846. doi: 10.1038/nprot.2012.116.

Shin, S., Wolgamott, L., Yu, Y., Blenis, J. and Yoon, S.-O. 2011. Glycogen synthase kinase (GSK)-3 promotes p70 ribosomal protein S6 kinase (p70S6K) activity and cell proliferation. *Proceedings of the National Academy of Sciences* 108(47). Available at: https://pnas.org/doi/full/10.1073/pnas.1110195108 [Accessed: 26 November 2024].

Siletti, K. et al. 2023. Transcriptomic diversity of cell types across the adult human brain. Science 382(6667), p. eadd7046. doi: 10.1126/science.add7046.

Simopoulos, A.P. 2002. The importance of the ratio of omega-6/omega-3 essential fatty acids. *Biomedicine & Pharmacotherapy* 56(8), pp. 365–379. doi: 10.1016/S0753-3322(02)00253-6.

Stahl, E.A. et al. 2019. Genome-wide association study identifies 30 loci associated with bipolar disorder. *Nature Genetics* 51(5), pp. 793–803. doi: 10.1038/s41588-019-0397-8.

Stark, D.T. and Bazan, N.G. 2011. Neuroprotectin D1 Induces Neuronal Survival and Downregulation of Amyloidogenic Processing in Alzheimer's Disease Cellular Models. *Molecular Neurobiology* 43(2), pp. 131–138. doi: 10.1007/s12035-011-8174-4.

Stoll, A.L. et al. 1999. Omega 3 Fatty Acids in Bipolar Disorder: A Preliminary Double-blind, Placebo-Controlled Trial. *Archives of General Psychiatry* 56(5), p. 407. doi: 10.1001/archpsyc.56.5.407.

Sun, Y., Liu, W.-Z., Liu, T., Feng, X., Yang, N. and Zhou, H.-F. 2015. Signaling pathway of MAPK/ERK in cell proliferation, differentiation, migration, senescence and apoptosis. *Journal of Receptors and Signal Transduction* 35(6), pp. 600–604. doi: 10.3109/10799893.2015.1030412.

Tyagi, S., Gupta, P., Saini, A., Kaushal, C. and Sharma, S. 2011. The peroxisome proliferator-activated receptor: A family of nuclear receptors role in various diseases. *Journal of Advanced Pharmaceutical Technology & Research* 2(4), p. 236. doi: 10.4103/2231-4040.90879.

Uhlén, M. et al. 2015. Tissue-based map of the human proteome. Science 347(6220), p. 1260419. doi: 10.1126/science.1260419.

Uzunova, G., Pallanti, S. and Hollander, E. 2016. Excitatory/inhibitory imbalance in autism spectrum disorders: Implications for interventions and therapeutics. *The World Journal of Biological Psychiatry* 17(3), pp. 174–186. doi: 10.3109/15622975.2015.1085597.

Watabe, T. and Miyazono, K. 2009. Roles of TGF-β family signaling in stem cell renewal and differentiation. *Cell Research* 19(1), pp. 103–115. doi: 10.1038/cr.2008.323.

Wei, Z., Li, D., Zhu, L., Yang, L., Chen, C., Bai, C. and Li, G. 2018. Omega 3 polyunsaturated fatty acids inhibit cell proliferation by regulating cell cycle in fad3b transgenic mouse embryonic stem cells. *Lipids in Health and Disease* 17(1), p. 210. doi: 10.1186/s12944-018-0862-x.

Wiktorowska-Owczarek, A., Berezińska, M. and Nowak, J.Z. 2015. PUFAs: Structures, Metabolism and Functions. *Advances in Clinical and Experimental Medicine* 24(6), pp. 931–941. doi: 10.17219/acem/31243.

Wilson, R.I. and Nicoll, R.A. 2002. Endocannabinoid Signaling in the Brain. *Science* 296(5568), pp. 678–682. doi: 10.1126/science.1063545.

Yamamoto, H. et al. 2023. GWAS-identified bipolar disorder risk allele in the FADS1/2 gene region links mood episodes and unsaturated fatty acid metabolism in mutant mice. *Molecular Psychiatry* 28(7), pp. 2848–2856. doi: 10.1038/s41380-023-01988-2.

Yang, X. et al. 2017. Serum fatty acid patterns in patients with schizophrenia: a targeted metabonomics study. *Translational Psychiatry* 7(7), pp. e1176–e1176. doi: 10.1038/tp.2017.152.

Zhang, Y.-P., Brown, R.E., Zhang, P.-C., Zhao, Y.-T., Ju, X.-H. and Song, C. 2018. DHA, EPA and their combination at various ratios differently modulated Aβ25-35-induced neurotoxicity in SH-SY5Y cells. *Prostaglandins, Leukotrienes and Essential Fatty Acids* 136, pp. 85–94. doi: 10.1016/j.plefa.2017.07.003.

Zhao, Y., Calon, F., Julien, C., Winkler, J.W., Petasis, N.A., Lukiw, W.J. and Bazan, N.G. 2011. Docosahexaenoic Acid-Derived Neuroprotectin D1 Induces Neuronal Survival via Secretase- and PPARγ-Mediated Mechanisms in Alzheimer's Disease Models. Smith, M. A. ed. *PLoS ONE* 6(1), p. e15816. doi: 10.1371/journal.pone.0015816.

Supplemental

1: FADS2 simple effects of gene expression by replication.

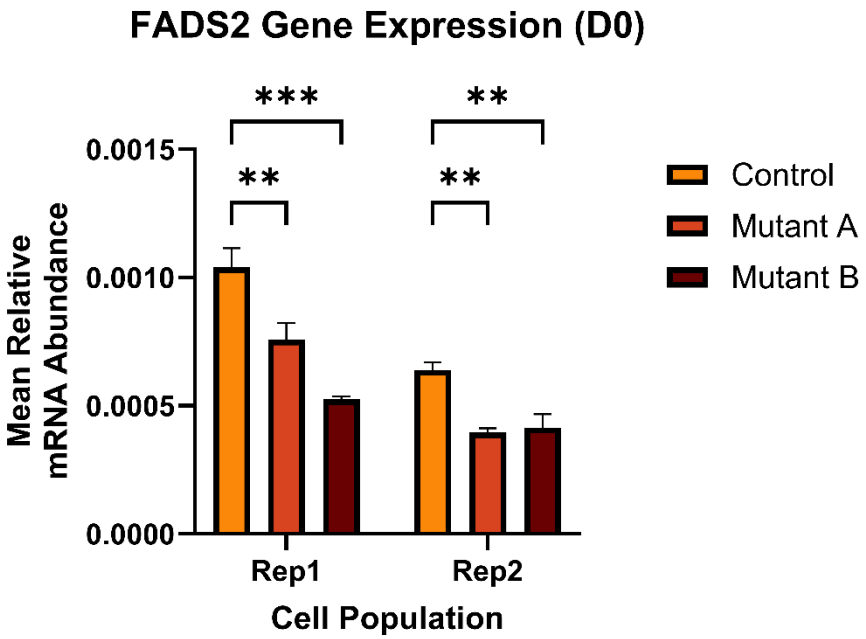

3: List of primers used for RT-qPCR

Gene	Forward	Reverse
ACTB	TCACCACGGCCGAGCG	TCTCCTTCTGCATCCTGTCG
DLG4	GGCACCGACTACCCCACAG	CACACCGTTGACCGACAGGA
FADS1	CGCTACTTCACCTGGGACGA	AAGGGATCCGTGGCATCCTG
FADS2	GGCGGGACCCTTTGTTTGTG	GAAGGCATCCTGTTGCCCG
FOXG1	AGGAGGGCGAGAAGAAGAAC	TCACGAAGCACTTGTTGAGG
GABRA1	GGATTGGGAGAGCGTGTAAAC AGGTGGGAGGAAAAGTCCTG	TGAAACGGGTCCGAAACTG TCATCATCTGCCTTATCAACACAGT
GAD1	GCCAGACAAGCAGTATGATGT	CCAGTTCCAGGCATTGTGTGAT
GRIA1	GGTCTGCCCTGAGAAATCCAG	CTCGCCCTTGTCGTACCAC
GRIA2	AGTTTTCCACTTCGGAGTTCAG	CCAAATTGTCGATGTGGGGTG
MAP2	AACCGAGGAAGCATTGATTG	TTCGTTGTGGGAAGCATTTCTCA
MCM2	GCGAAACCTGGTTGTTGCTGT	AGGATTCCGATGATTCCGCC
MKI67	TCCTTTGGTGGGCACCTAAGACCTG	TGATGGTTGAGGTCGTTCCTTGATG
NANOG	ACGCAGAAGGCCTCAGCACCT	CCCAGTCGGGTTCACCAGGCA
NES	AGCAGGAGAAACAGGGCCTAC	CTCTGGGGTCCTAGGGAATTG
PCNA	CCGGTTACTGAGGGCGAGAAG	ACCGGCTGAGACTTGCGT
POU5F1	TTCTGGCGCCGGTTACAGAACCA	GACAACAATGAAAATCTTCAGAGAGA

PTGS1	CTGTTCCTGCTCCTGCTCC	CACAGGCCAGGGATGGTG?
PTGS2	GCCATGGGGTGGACTTAAATCAT	CCACAGCAAACCGTAGATGC?
SYT1	TCATCTGATGCAGAATGGTAAGAGG	GTAGCCCACAAAGACTTTGCC
TUBB3	CATGGACAGTGTCCGCTCAG	CAGGCAGTCGCAGTTTTCAC